

Comparing electric vehicle charging strategies in stochastic microgrid optimization

Markos Wahid

Master of Science Thesis

Comparing electric vehicle charging strategies in stochastic microgrid optimization

MASTER OF SCIENCE THESIS

For the degree of Master of Science in Systems and Control at Delft
University of Technology

Markos Wahid

September 20, 2019

Faculty of Mechanical, Maritime and Materials Engineering (3mE) · Delft University of
Technology



The work in this thesis was supported by Stedin. Their cooperation is hereby gratefully acknowledged.



Copyright © Delft Center for Systems and Control (DCSC)
All rights reserved.

Abstract

Renewable energy sources, e.g. solar energy and wind energy, have gained popularity as an alternative means of energy production as they do not reinforce global warming. In addition, more and more electrical appliances (e.g. electric vehicles, induction cookers, and heat pumps) are used as a substitute for appliances that need non-renewable energy sources.

This increase in the use of renewable energy resources pushes the electricity grid to its limits due to new induced load peaks. The grid is not designed for these developments and as a result, asset deterioration, higher transport losses, and outages are expected to occur. The most straightforward solution for the distributed system operator, i.e. the operating manager of the distribution network, is to expand the grid. However, grid expansion is a costly operation and there are additional promising methods to decrease grid load peaks, e.g. by using different charging strategies for electric vehicles.

The conventional charging strategy for electric vehicles is uncontrolled charging. With uncontrolled charging, the charging of the electric vehicle immediately commences once a connection with the charging pole is established. The smart charging strategy, however, is able to delay the charging moment to a more optimal time instant in view of, e.g. variable electricity prices. The vehicle-to-home (V2H) charging strategy is similar to smart charging, but in addition, V2H charging allows the electric vehicle to discharge electricity to power a nearby household.

This research aims to compare smart charging and V2H charging on their economical effects for their users. The charging strategies are implemented using two control algorithms: a rule-based controller and a model predictive control (MPC) algorithm. The rule-based controller is implemented due to its simplicity and the MPC algorithm is used for its ability to take into account predictions of system related variables, e.g. household loads. The MPC algorithm is implemented with two different forecasts namely, perfect information, i.e. uncertain variables are forecasted perfectly, and certainty equivalent, i.e. uncertain variables are predicted using a persistence forecast model. The persistence forecast model assumes that future values of an uncertain variable remain equal to the latest measurements, e.g. the solar generation of tomorrow is expected to be equal to that of today. The control problem is non-linear as an electric vehicle behaves differently depending on its status, e.g. driving or charging. The control problem is therefore reformulated into a mixed logical dynamical framework such that

it can be solved efficiently using mixed integer linear programming. An extensive comparison in performance for a microgrid case study is done using real data of solar generation, electric vehicles, and household loads for simulation. The results show that the V2H charging strategy can outperform smart charging by reducing both the peak loads and the electricity costs. However, the V2H strategy only gives a minor extra decrease in costs compared to smart charging and the performance of V2H charging is highly dependent on the quality of the forecasts. Therefore, it is concluded that, in practice, smart charging is the most effective charging strategy.

Further research is done to investigate whether the microgrid costs, using a smart charging strategy, can be reduced further by taking into account the uncertainty of some variables such as the electricity price and the household load. This is implemented through a scenario-based MPC algorithm due to its ability to incorporate multiple forecasts, i.e. scenarios, for each uncertain variable. Six different scenario generation methods are implemented which are distinguished by two characteristics: the period from which the historical error between the certainty equivalent case and the true realization of the uncertain variable is collected (i.e. yearly, seasonal, or daily) and the addition method of these errors to the persistence forecast model to generate new scenarios, i.e. as a variable or as a constant. An extensive comparison in performance for a microgrid case study is done. The results show that the certainty equivalent MPC case can be outperformed if a low number of scenarios is generated. This is achieved most effectively by collecting the persistence forecast model error from a rolling horizon of the past 24 hours and adding the error as a constant to the persistence forecast model.

Table of Contents

| | |
|--|----------|
| Acknowledgements | v |
| 1 Introduction | 1 |
| 1-1 Energy transition | 1 |
| 1-1-1 Motivation | 1 |
| 1-1-2 Consequences for the distributed system operator | 2 |
| 1-1-3 Potential solutions | 3 |
| 1-2 Research objective | 4 |
| 1-3 Contributions | 4 |
| 1-4 Outline | 4 |
| 2 Microgrids and components description | 5 |
| 2-1 Microgrids | 5 |
| 2-1-1 Challenges | 6 |
| 2-1-2 Control | 7 |
| 2-1-3 Economical costs | 9 |
| 2-2 Electric vehicles | 11 |
| 2-2-1 Motivation | 11 |
| 2-2-2 Charging strategies | 11 |
| 2-2-3 Battery degradation | 14 |
| 2-2-4 Travel profile of electric vehicles | 16 |
| 2-3 Photovoltaic generation | 18 |
| 2-4 Household loads | 19 |
| 2-5 Conclusions | 21 |

| | | |
|----------|--|-----------|
| 3 | Microgrid modelling and control | 23 |
| 3-1 | Microgrid modelling | 23 |
| 3-1-1 | Power equilibrium | 23 |
| 3-1-2 | Economical costs | 24 |
| 3-2 | Electric vehicle modelling | 24 |
| 3-2-1 | Battery dynamics | 24 |
| 3-2-2 | Charge power limitation | 25 |
| 3-2-3 | Range anxiety | 26 |
| 3-2-4 | Battery degradation constraint | 26 |
| 3-2-5 | Varying properties | 26 |
| 3-3 | Mixed logical dynamical framework | 26 |
| 3-4 | Rule-based control | 28 |
| 3-5 | Model predictive control | 29 |
| 3-5-1 | General description | 29 |
| 3-5-2 | Microgrid implementation | 31 |
| 3-5-3 | Scenario-based | 32 |
| 3-6 | Scenario generation | 32 |
| 3-6-1 | Historical forecast error methods | 32 |
| 3-6-2 | Matching profile method | 35 |
| 3-7 | Conclusions | 36 |
| 4 | Simulation and results | 39 |
| 4-1 | Case study introduction | 39 |
| 4-2 | Case study 1: comparing electric vehicle charging strategies | 41 |
| 4-2-1 | Results | 42 |
| 4-2-2 | Conclusions | 45 |
| 4-3 | Case study 2: comparing scenario generation strategies | 46 |
| 4-3-1 | Results | 47 |
| 4-3-2 | Conclusions | 49 |
| 4-4 | Conclusions | 49 |
| 5 | Conclusions and recommendations | 51 |
| 5-1 | Summary and conclusions | 51 |
| 5-2 | Discussion and future work | 52 |
| 5-3 | Advice to distributed system operator | 53 |
| A | Reformulation of electric vehicle battery dynamics | 55 |
| | Glossary | 61 |
| | List of acronyms | 61 |
| | List of symbols | 61 |

Acknowledgements

Receiving my Master of Science degree from the TU Delft feels like a dream. As a high school student, I would never have thought I would reach up to this point, certainly since I started at pre-vocational secondary education (VMBO). Trough the motto: nothing ventured, nothing gained, and with the support of friends and family I am grateful that I have reached this milestone. Doing this research had its ups and downs, this is confirmed physically as my first gray hairs appeared during this period. Luckily, I was not on my own and this section is used to acknowledge the people who supported me throughout this research.

This research is done in collaboration with the Dutch distributed system operator Stedin. The collaboration was very valuable due to the available data and for having a business perspective in this research. In addition, I was able to visit transformer stations and the operating center through which I have learned a lot about the electric power distribution network. Therefore, I would like to thank my Stedin supervisors Arjan van Voorden and Henk Fidder for their guidance and giving me the opportunity to collaborate. My fellow Stedin interns are also much appreciated for the interesting discussions about our research during the lunch walks outside.

Furthermore, I would like to acknowledge my daily supervisor Tomás M. Pippia who was always available for questions when needed. His explanations of, e.g. model and control techniques, and the proofreading of this report were invaluable. Moreover, I would like to thank prof.dr.ir. Bart De Schutter for the efficient meetings and for guiding my research progress.

Next, I would like thank my friends which are known as the Vaggaboy for the great fun times we had (and still have) while living together in The Hague.

A special thanks to my mother, sister, and father who have supported me throughout my whole life to obtain my university degree. In addition, I would like to thank my family in England and Germany who are always cheering me on.

Finally I would like to show my gratitude to my girlfriend Loesie Willemsen. She helped me keep my sanity during challenging periods through giving love, care, and compassion. Furthermore, her patience is much appreciated as a lot of my time was devoted to this research. She also taught me the skill of juggling during my thesis which helped to take my

mind off from doing research when I needed a break.

Delft, University of Technology
September 20, 2019

Markos Wahid

“Whether you think you can, or you think you can’t — you’re right.”

— *Henry Ford*

Chapter 1

Introduction

This chapter serves as an introduction to this thesis work. The energy transition is presented in Section 1-1 as context for the research problem. Next, the research objective is discussed after which the contributions in this thesis are highlighted in Section 1-2 and Section 1-3 respectively. Lastly, an outline of this report is given in Section 1-4.

1-1 Energy transition

This section introduces the energy transition as context of this research. First a description is given of why society is assisting to an energy transition. Thereafter, the potential negative effects for the distributed system operator (DSO) are discussed after which potential solutions are presented.

1-1-1 Motivation

Fossil-fuel generation technologies have been the most common choice for the generation of electricity due to their scalability, competitive investment costs, and flexible operation. A disadvantage of using non-renewable energy sources is that its supply is limited while the energy demand of the world is rising. In addition, using non-renewable energy sources releases carbon dioxide in the atmosphere that increases the greenhouse effect. The greenhouse effect causes an increase of the mean temperature of the earth, i.e. global warming, which results in rising sea levels, more frequent extreme weather events, and the expansion of deserts [34]. Renewable energy sources, e.g. solar and wind energy, do not have the aforementioned negative effects and are therefore used more and more as an alternative energy source.

In addition, fossil fuel powered appliances are increasingly replaced by electrical appliances, e.g. boilers are replaced by heat pumps, combustion engine vehicles are replaced by electric vehicles (EVs), and gas stoves are replaced by induction stoves. The increase in EV adoption is highlighted in Figure 1-1 where the expected number of EVs in the future in the Netherlands

is shown in three different policy and development scenarios: European regional policies (line), national policy (dashed), and fast technological developments (dotted) [1]. Consequently, a strong rise in the consumption of electricity is expected in the future.

The structural power system change discussed in this section, i.e. using more renewable energy sources instead of fossil-fuels, is also known as the energy transition.

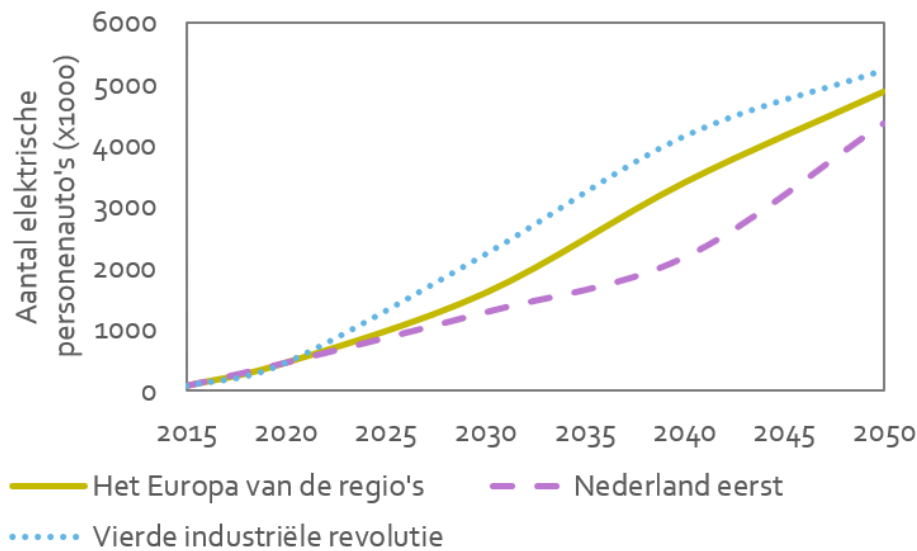


Figure 1-1: Estimated number of EVs [$\cdot 1000$] (y-axis) in a future year (x-axis) in the Netherlands [1].

1-1-2 Consequences for the distributed system operator

It is expected that the increase in electricity demand will cause grid overcapacity problems in the future. These grid problems are partially due to the charging of EVs during peak demand. For instance, the Nissan Leaf (2018) has a 40 kWh battery pack of which the amount of electricity required to charge it fully, accounts to roughly the same amount of electricity as four households would use in Netherlands each day. Furthermore, households have a daily cyclic electricity demand profile with a load peak at the end of the day as shown in Figure 1-2. This load peak is around the time when most people return home from work and start e.g. cooking dinner and watching tv. This load peak will increase significantly if households also charge their EVs during that time.

If the additional loads are not appropriately controlled, the aging of the power system will be accelerated due to e.g. overheating power transformers. Furthermore, it is estimated that 30% EV adoption will cause capacity problems and critically low voltages in Dutch city centers from 2030 onwards [27, 36].

On the other hand, overcapacity on the grid can also be due to solar and wind peak production. From 2020 a "Nul op de Meter", a Dutch term for self-sufficient energy households, living area will have bottle-necks in the grid due to high photovoltaic (PV) energy production resulting in problematic high voltage levels [17].

The expected grid problems are not only a concern for the DSO who is responsible for facilitating and maintaining the electric power distribution system. Households pay the DSO a monthly fee for facilitating a connection with the main grid and if the capacity of the connection needs to increase, higher monthly fees must be paid to the DSO [32]. Furthermore, the increased asset maintenance costs will eventually be passed on to the households through higher DSO fees. The expected grid problems are therefore also a concern for the households.

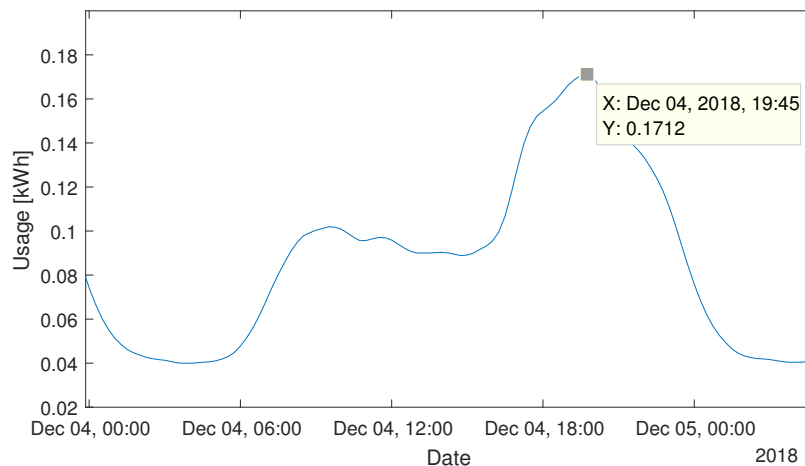


Figure 1-2: Estimated two-person Dutch household electricity load profile (E1A) in winter 2018 [17, 22].

1-1-3 Potential solutions

There are multiple possible solutions to mitigate the voltage and capacity problems of the DSO. The most straightforward solution is to expand the grid capacity through adding extra cables in the ground, however, this is a costly operation. Furthermore, a controllable transformer can mitigate voltage and capacity problems through adapting the number of windings on the primary or secondary coil. However, this solution does not work when critical low and high voltage occur simultaneously on different feeders to the same transformer.

The grid problems can also be mitigated through the electricity production side using curtailment. Curtailment is the reduction of the output from an energy source such that it produces less than its maximum production rate. Curtailment is typically employed in an involuntary basis as it results in a lower production output. However, a compensation to the energy producers could be given for lost turn-over. On the other hand, flexible loads can mitigate grid problems from the demand side through controlling the electricity demand. For instance, instead of charging the EV immediately when people arrive home, the EV could use a different charging strategy, e.g. charging in the middle of the night. Another example of flexible loads are smart controlled heat pumps, however, it has less electrical flexibility compared to EVs. Finally, home or district batteries can also be used to mitigate grid problems, still, this is not a competitive solution due to the related investment costs [36]. An additional advantage for the owners of the flexible loads is that electricity can be bought for potential cheaper rates through a variable electricity price.

1-2 Research objective

As discussed in the previous section, the expected increase of EV adoption is likely to create grid problems for the DSO. Using the EVs as flexible load could mitigate these problems while possibly lowering the economic costs for the owners. Therefore, this thesis compares several EV charging strategies, i.e. uncontrolled charging, smart charging, and vehicle-to-home (V2H) charging, on their economical effects for their users in a microgrid. Additional research is done to investigate whether the total microgrid costs, using smart charging, can be reduced further through taking into account the uncertainty of some variables, i.e. the PV generation, the electricity price, and the household loads.

1-3 Contributions

This research aims to depict reality as close as possible without making the microgrid model too complex. This is achieved through using real data of EV charging pole arrival and departure times, PV generation, household loads, and variable electricity prices and through simulating a case study for different seasons. Furthermore, the rule-based control algorithm discussed in Section 3-4 and the scenario generation methods discussed Section 3-6 are developed by the author.

1-4 Outline

This report starts with a description of microgrids, EVs, PV generation, and household loads which will act as fundamental background knowledge for this report in Chapter 2. The modeling of microgrids and EVs together with several control methodologies, i.e. rule-based, model predictive control (MPC), and scenario-based MPC are presented in Chapter 3. The simulations of two case studies and their results are discussed in Chapter 4. Lastly, Chapter 5 presents the final conclusions of this research together with some points for discussion, suggestions for further research, and advise to the DSO.

Microgrids and components description

This chapter introduces several topics related to microgrids that will be useful throughout the thesis. In Section 2-1, the advantages and the related challenges for the use of microgrids are described. In addition, the hierarchical control structure of the microgrid and the economical costs are introduced. The electric vehicle (EV) is described with its advantages, different charging strategies, and battery degradation in Section 2-2. Furthermore, the travel profile of EV owners is also highlighted. Finally, photovoltaic (PV) generation and household load profiles and their seasonal patterns are discussed in respectively Section 2-3 and 2-4.

2-1 Microgrids

The electricity grid connects a large number of distributed energy resources, i.e. energy sources (renewable and non-renewable), energy storage systems (e.g. hot water tank or batteries), and controllable loads (e.g. EVs or washing machines) together. Controlling a big number of distributed energy resources in a reliable, efficient, and safe way is a challenging objective. This control burden on the main grid can be mitigated by connecting and controlling the distributed energy resources in smaller networks, i.e. microgrids. Microgrids give therefore rise to a more decentralized controlled electricity grid.

In addition, distributed generation of energy has several advantages [14]. In the first place, the opportunity arises to locally utilize waste heat for district heating, e.g. gas turbines. Furthermore, the presence of generation close to demand can increase the power quality and the reliability of electricity. Finally, reduced line losses are achieved, since the distance between the energy source and its user is generally shorter using distributed generation compared to centralized generation, .

The microgrid and the main grid are usually connected through a point of common coupling (PCC). If such a connection is interrupted, e.g. intentionally or incidentally, or if it

does not exist at all, the microgrid is addressed as isolated or islanded. Islanded microgrids are not a new concept as they have already existed for several decades in remote communities where the interconnection with the main power grid was not feasible due to technical or economical reasons [24]. Islanded microgrids are mentioned only for the sake of completeness as the concept falls outside the scope of this research.

2-1-1 Challenges

The mentioned advantages in the previous section, e.g. reduced line losses, clearly depict the potential of microgrids. In this section however, several challenges are addressed which need to be taken into account such that a microgrid can operate safely due to, e.g. complex control of distributed energy resources and deviations of voltage and frequency [24, 31].

The control complexity in a microgrid increases due to the need of power electronic converters. The power electronic converters accommodate a safe connection between different energy resources, which either operate on alternating current (AC) or direct current (DC). The connection of DC-type energy sources, e.g. PV panels, EVs, and energy storage technologies, requires the use of a DC-to-AC power converter interface. Some conventional generators can be connected directly to the microgrid, however, variable-speed generators, e.g. wind turbines, require the use of AC-to-AC power converters to match the constant frequency and voltage of the microgrid. Loads within the microgrid can be controlled using either a conventional circuit breaker or a more sophisticated AC-to-AC power electronic interface to allow more flexible control. Figure 2-1 illustrates that a power electronic converter is needed for almost each implemented distributed energy resource.

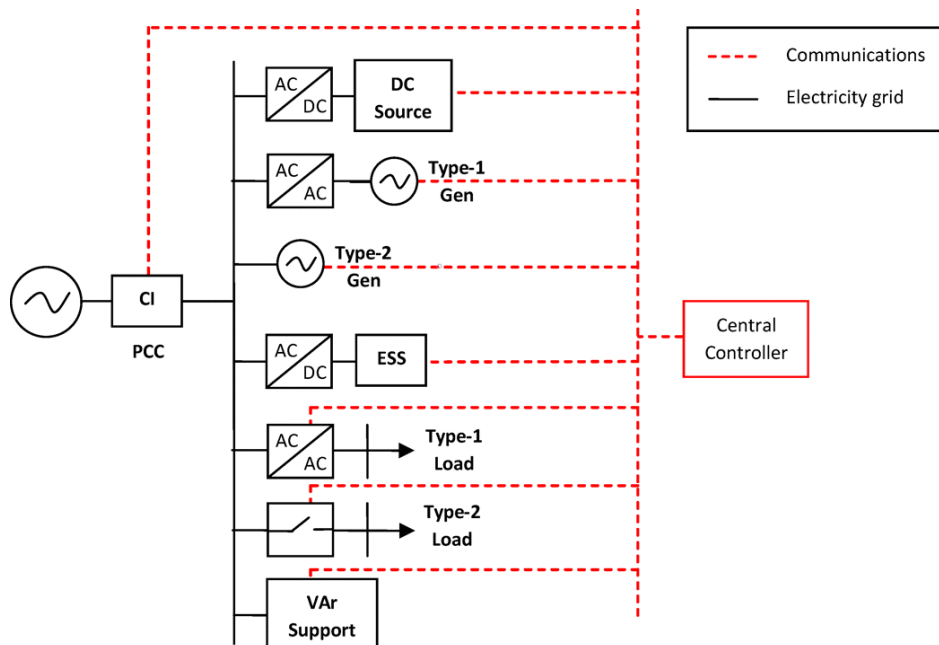


Figure 2-1: Microgrid with several distributed energy resources in a schematic overview including an ESS and a VAr support, i.e. reactive power support [24].

Moreover, severe voltage and frequency deviations can occur due to low availability of rotational inertia. The voltage and frequency instabilities occur when there is a mismatch between power generation and consumption. When the demand for active power increases in a AC grid, the frequency will fall and vice-versa. Similar relations are observed regarding reactive power and voltage. Equipment failure, distorted power quality, and stability problems are possible consequences of having fluctuations in system voltage and frequency [31].

Finally, there is more uncertainty in microgrid systems compared to larger networks due to limited averaging effects of stochastic variables, e.g. household loads and solar generation. The increased uncertainty makes it more difficult for a control algorithm to employ safe, efficient, and reliable control in a microgrid.

These challenges require a proper microgrid control architecture which is the main topic in the subsequent section.

2-1-2 Control

There are several controllers in a microgrid, each having different objectives, see [4] and the references therein. Altogether they contribute to having a reliable, sustainable, and economically efficient working microgrid due to the realization of the following functionalities:

- Voltage and frequency regulation
- Proportional active and reactive power-sharing
- Microgrid resynchronization with the main grid
- Power flow control between the microgrid and the main grid
- Unit commitment problem, i.e. choosing the best subset of distributed energy sources to share the loads
- Economic dispatch, i.e. optimizing the microgrid operation cost in a future time period
- Demand side management

The listed requirements are of different time scales. Microgrid control is therefore generally implemented in a hierarchical structure (considering a single microgrid). The controller types are usually divided into three control layers: primary, secondary, and tertiary.

Primary and secondary control

The voltage and frequency in the microgrid are stabilized through primary control [4]. In addition, the primary control offers plug and play capabilities for distributed energy resources and the sharing of active and reactive power between them. The power-sharing mitigates circulating currents that can cause excessive heat generation in the power electronic devices. Primary control provides reference points to the voltage and current control loops of distributed energy resources which are commonly referred to as zero-level control.

Using only primary control is insufficient as it may cause frequency deviations even in steady state. Secondary control restores the microgrid voltage and frequency and compensates the remaining deviations due to the primary control. It has a sampling time from seconds to minutes and is slower than primary control.

Primary and secondary control fall outside the scope of this research. It is assumed that the voltage and frequency deviations in the microgrid are successfully controlled by the primary and secondary control layers as the main interest of control in this research is in the third control layer.

Tertiary control

Tertiary control is carried out by an energy management system (EMS) which solves the economic dispatch and unit commitment problem [23]. The constraints that the EMS has to consider are associated with the operational limits of the generating units, power flow, and energy balance in the grid, see Figure 2-2. In addition, ramping-rates, minimum-up/minimum-down times, start-up/shut-down times, intermittent renewable energy sources, and intermittent non-dispatchable energy resources also have to be dealt with appropriately. The sampling time of an EMS ranges from minutes to hours.

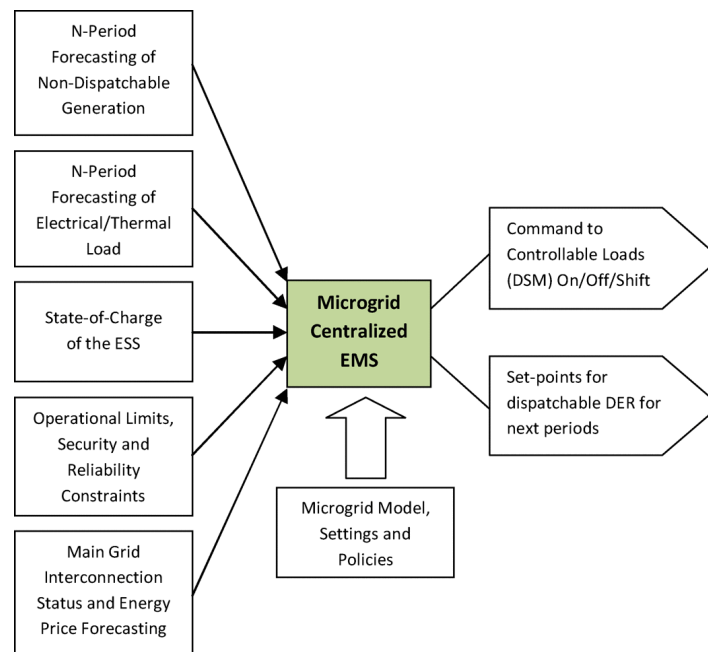


Figure 2-2: Centralized approach to tertiary control of microgrids (DSM = demand side management) [24].

Energy management systems have the primary focus in this research as the tertiary control level is the most appropriate level for implementing vehicle-to-everything (V2X) charging strategies. Numerous energy management systems methods exist such as multi agent control, rule-based control, and model predictive control (MPC) [31]. The optimization-based approach MPC is an interesting strategy since it has the possibility to account for uncertainties

and constraints in a pre-defined future time horizon. Rule-based control often gives inferior control performance compared to MPC. However, rule-based control is easy to implement, especially compared to MPC, therefore it is used as performance benchmark. More information about rule-based control and MPC can be found in Section 3-4 and Section 3-5 respectively.

2-1-3 Economical costs

This section presents the financial costs due to electricity usage in the Netherlands. The height of the financial costs will be affected by the implemented EV charging strategy in a microgrid and is therefore important to consider for households. The economical costs consist of the variable price for electricity usage which is paid to the electricity supplier, the costs for the use of the electricity grid which is paid to the distributed system operator (DSO), and taxes.

Tax on energy use is imposed by the Dutch government to discourage excessive energy usage and to defray the government expenses of stimulating green energy technologies [2]. The taxes are based on the total amount of purchased electricity in a period. The implemented charging strategies in this research possibly only have a minor effect on the total quantity of electricity demand due to efficiency losses as elaborated in Section 4-2-1. Taxes are therefore disregarded as economical costs in this research since the tax difference between charging strategies will be insignificant and is not expected to affect the drawn conclusions after microgrid simulations.

Electricity price

The end user costs of the electricity received from electricity supplier are based on the purchase costs of electricity by the electricity supplier from the day-ahead market. The day-ahead market, is a platform where large scale electricity producers and consumers, e.g. electricity suppliers or large industrial companies, can trade electricity for a specific hour the next day [5].

How the electricity supplier resells the bought electricity from the day-ahead market to its clients is unclear as this is arranged through private contracts with large consumers, i.e. consumers with connections larger than $3 \cdot 80$ A. It is expected that the electricity supplier resells the electricity from the day-ahead market to its clients for its original price with the addition of overhead costs from the electricity supplier.

In this research, the day-ahead market price is assumed to be the price that the households in the microgrid have to pay. This is due to the expectation that the day-ahead market price is the biggest driver of the end consumer price. In addition, the day-ahead market price of a specific hour is only assumed to be known by the microgrid at that specific hour, i.e. the price is not known one day ahead. Furthermore, only large consumers are considered in this research as small consumers, i.e. consumers with connections smaller than or equal to $3 \cdot 80$ A, do often not have or only have minor variable prices for which the potential economical costs savings are insignificant.

When analyzing the 2018 year data of the day-ahead market price [10], shown in Figure 2-3 no seasonal, e.g. summer or winter, characteristics are visible. However, on a weekly scale, a daily cyclic pattern is recognized. Figure 2-4 shows the weekly prices of 2018 plotted over each

other and the mean profile is also shown. It is observed that an increase in electricity demand correlates with an increased electricity price, see Section 2-4 and compare with Figure 2-14.

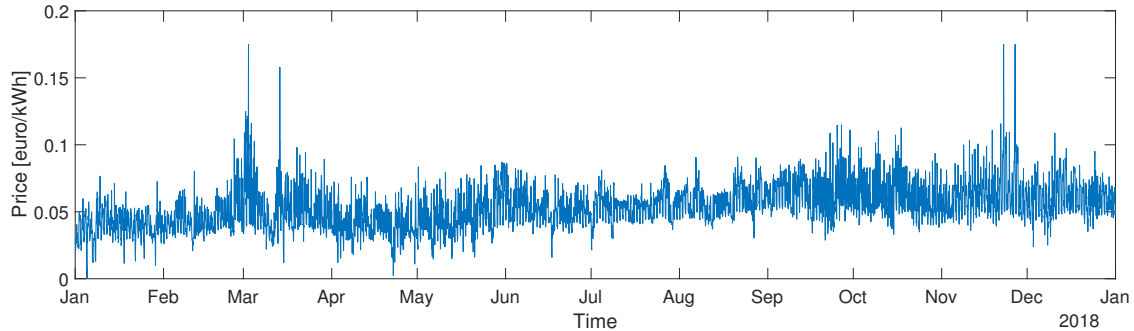


Figure 2-3: Day-ahead market price.

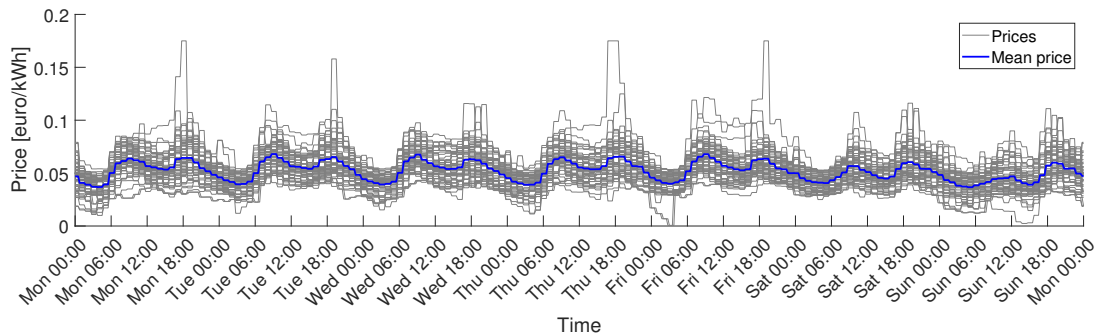


Figure 2-4: Weekly day-ahead prices together with the mean profile.

Currently in the Netherlands, there exists an electricity usage balance regulation which stipulates that the amount of excess generated electricity, e.g. due to PV generation, can be subtracted from your yearly electricity demand. In principle, electricity can be sold back to the main grid for the purchase price as long as the yearly electricity demand is higher than the generated amount of electricity. However, the Dutch government has plans to change this regulation in the future such that a much smaller price is received for selling electricity. As a result, the plans will make selling electricity back to grid less profitable than before. It is uncertain how the electricity selling price will differ from the purchase price in the future, however it is expected that this difference will not be small. It is assumed in this research that the selling price will be half of the electricity purchase price.

Distributed system operator costs

The economical costs of the DSO are mainly driven by the peak power demand to the grid [33]. The peak power demand to the grid determines the size of the physical connection needed for which fixed periodic costs have to be paid. In addition, an extra fee is paid for the monthly peak power demand. Depending on the connection type, an additional fee is paid for the total amount of demanded energy. Every client pays the fixed connection

fees, however, clients do not have to pay a fee for the peak power and exchanged energy of electricity that is generated and fed back into the grid.

2-2 Electric vehicles

Several EV related topics are presented in this section. First of all, a description of the economic benefits of EVs is given. Several charging strategies are introduced thereafter such as uncontrolled charging and V2X charging. Subsequently, the topic of EV battery degradation is addressed. Lastly, the driving patterns of EV users are presented with the focus on the yearly driven distances and charging pole arrival and departure times. It is important to note that hybrid electric vehicles are not considered in this work and that the term EV only refers to full battery electric vehicles.

2-2-1 Motivation

Important incentives for households to own EVs are cheaper charging rates and the possibility to charge only from electricity generated from renewable energy sources. The sustainable motivations of society are clear due to the energy transition explained in Section 1-1-1. Therefore, an economical motivation for EV adoption is presented in this section.

Several advantages are identified of the electric motor compared to a conventional combustion engine [9]. Firstly, the purchase costs of an electric motor per kilowatt are less than 50 % of the purchase price of a gasoline-powered engine. In addition, due to further developments of the electric motor it is expected that the current price will be reduced with 50 % in 2035. As the development of the combustion engine is mature, the expected improvements are limited. Supposedly, there are a lot of improvements on CO₂ emissions tested by the New European Driving Cycle [35]. However, the actual improvements tested on the road proved to be limited.

Furthermore, the maintenance costs of an electric powertrain are around one-third of the costs of maintaining a combustion engine powertrain. These costs will reduce even further when EVs become a more common means of transport. Moreover, the energy use of an electric motor is on average less than a third of the energy needed with a combustion engine.

Although the total cost of ownership savings on the electric motor are substantial, the biggest savings come from the fuel costs. Gasoline production and delivery costs are approximately 6 cents compared to 7 cents (excluding electricity connection fees) for electricity per kWh. Dutch taxes increase the prices up to 17 and 19 cents for gasoline and electricity respectively [9]. However, since the EV needs three times less energy, the energy costs per kilometer are 13 and 4 cents for gasoline and electricity respectively. Thus resulting in a saving of more than 200 euros each month when driving twenty thousand kilometers per year.

2-2-2 Charging strategies

This section presents an extensive analysis on different charging strategies since this is a fundamental topic in this thesis. The uncontrolled charging strategy is discussed first after which V2X charging, e.g. smart charging and vehicle-to-home (V2H) charging, is elaborated.

Uncontrolled charging

Currently, most EVs are charged in an uncontrolled way. That is, when the EV is connected to the charging pole, charging immediately commences and stops when the battery of the electric vehicle is full.

Charging EVs is always associated with an energy loss due to AC-to-DC power conversion as discussed in Section 2-1-1. A power converter efficiency of 90 % is assumed in this research [16].

Uncontrolled charging of lithium-ion (Li-ion) batteries, used in most EVs, is often done with a constant current, constant voltage, and trickle charge mode respectively [37], see Figure 2-5. In constant current mode, the battery is charged with an increasing voltage and constant current. When the battery voltage reaches a specific value, the mode is switched to constant voltage where the voltage is kept constant while the current is reduced. Constant voltage mode is used to charge the battery until it is full while preventing overcharging the battery. The final mode, trickle charging, ensures to compensate the self discharge of the battery after the battery has been charged fully. The charging mode changes depending on the state of charge (SOC), i.e. the percentage of remaining energy, of the battery and affects the charge power. The largest segment of the battery is charged in constant current mode and the remaining smaller segment in constant voltage mode. The charge duration in both modes however, is approximately the same or even longer for constant voltage mode.

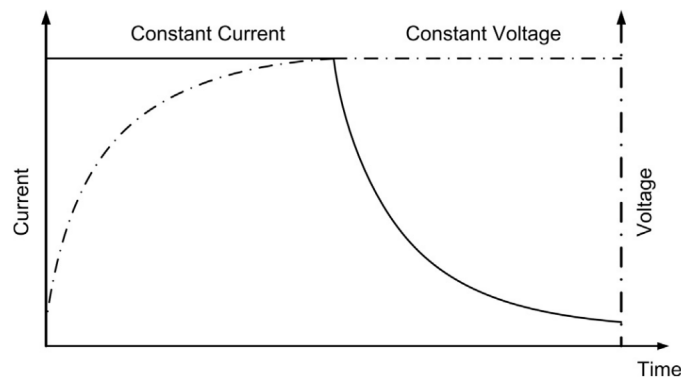


Figure 2-5: Uncontrolled charging profile EV with Li-ion battery [37].

Figure 2-6 shows the relationship between the SOC and the uncontrolled charge power in which the constant current and constant voltage modes can be distinguished. When focusing on the 400 V, i.e. three-phase, charging sessions, the battery charging power increases gradually from 0 % to approximately 25 % SOC, i.e. constant current mode. Then from 30 % to 87.5 % SOC, a marginally constant power profile is recognized. The remaining SOC is observed to resemble a negative linear correlation with the charge speed, i.e. constant voltage mode.

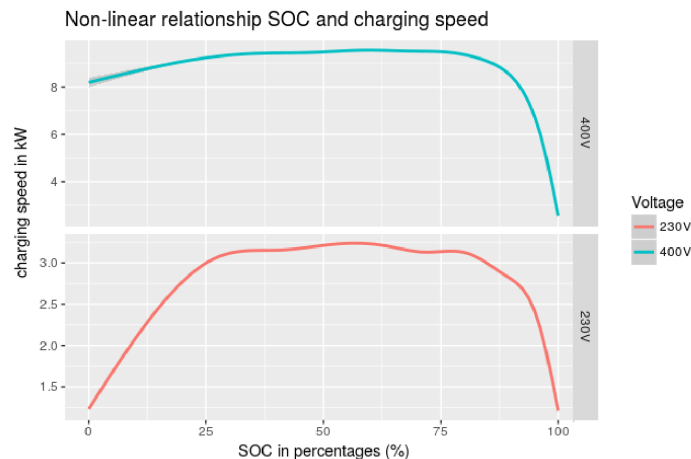


Figure 2-6: SOC and charge profile relationship for one and three phase charging [19].

The SOC dependency discussed in this section is used to develop a model for uncontrolled charging of EVs in this thesis. The first slowly rising power part up to 25 % SOC in Figure 2-6 is not modeled as EVs generally do not arrive with completely empty batteries. The uncontrolled power profile is thus assumed to be constant from 0 % up to 87.5 % SOC. Constant voltage mode cannot be ignored as it strongly effects the charge duration of the remaining part of the SOC. This is taken into account through modelling the constant voltage mode as a linear power decline from 87.5 % up to 100 % SOC. The maximum EV charge power is chosen as 11 kW in this thesis which is based on the analysis of three phase charging pole data [28].

Vehicle-to-everything charging

The increase in of EV adoption while using an uncontrolled charging strategy will create higher peak demands which is problematic for the DSO, see Section 1-1-2. However, EVs can also be employed to mitigate potential grid problems. Using an EV as dynamic load, dynamic energy storage system by feeding power to the electric grid, and for ancillary services (i.e. peak power shaving, spinning reserve, voltage, and frequency regulations) is referred to as vehicle-to-grid (V2G) charging. A single EV has a negligible effect on V2G services. Therefore, a large number of EVs is generally aggregated for employment of V2G charging. The aggregator gathers information about the market situation and schedules charging and discharging according to expected revenues [11]. The revenues are then distributed to the EV owners according to a predetermined contract. The EV aggregator maintains the link between energy market players and EV owners. In addition, the aggregated EV integration can be conceived as a virtual power plant in which EVs are clustered and controlled as a single energy source. The aggregated flexible employed EVs can also act as an energy storage system which will accelerate the integration of renewable energy sources, e.g. the use of PV panels on the roof of parking lots to contribute to the charging of EVs. Adopting regular energy storage systems, e.g. home batteries, involves high investment costs which hinders the adaption of renewable energy sources.

The term V2G refers to employing EVs with the main purpose to alleviate grid problems.

Other charging strategies exist which have other main goals, e.g. vehicle-to-vehicle (V2V) and V2H. All these controlled EV charging strategies are captured under the umbrella term V2X. The aim in this research is to employ the EVs to reduce the economical costs for its owners and households in the microgrid, the effects on the main grid are outside the scope of this research. Two V2X charging strategies are considered in this thesis which are best suitable for reducing the economical microgrid costs for households namely smart charging and V2H.

The smart charging strategy controls the charge power flow profile to the EV in terms of time and intensity and is a unidirectional process, i.e. the EV can only be charged. The V2H charging strategy is similar to smart charging, but in addition, V2H charging allows to discharge the EV to provide electricity to a nearby household. An advantage of V2H charging is that it allows the EV to act as an energy storage system, e.g. store excess generated PV energy in the midday and use the electricity to power a household in the evening. The goals of smart charging and V2H charging are to decrease the economical costs of the microgrid through reducing the economical microgrid costs and have a fully charged EV upon departure from the charging pole.

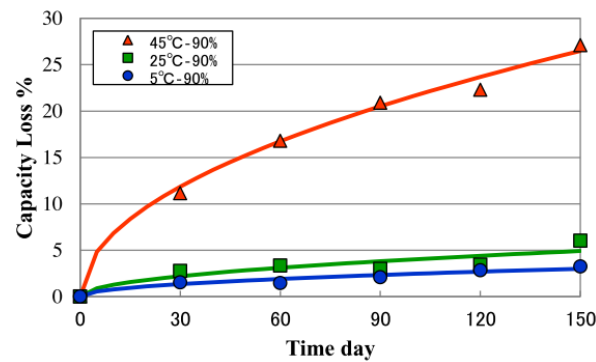
Although the potential advantages of V2X charging are promising, EV owners have doubts and concerns for the following reasons. While using V2X charging, it might be valuable to postpone charging or even to reduce the SOC if the current electricity prices are high [11]. This idea gives the fear to users that the battery is not sufficiently charged when the user needs the EV, i.e. range anxiety. Another concern is that the battery life is shortened when controlled bi-directional charging is used and that V2X charging restricts the freedom and independence of EV users. The EV aggregator should tailor the charging strategies to customer needs to increase the participation in V2X charging. Furthermore, implementation of V2H charging is not straightforward due to bidirectional power flows in the charging pole and in the EV. Most currently available commercial EVs do not support bidirectional charging, which brings extra investment and implementation costs.

2-2-3 Battery degradation

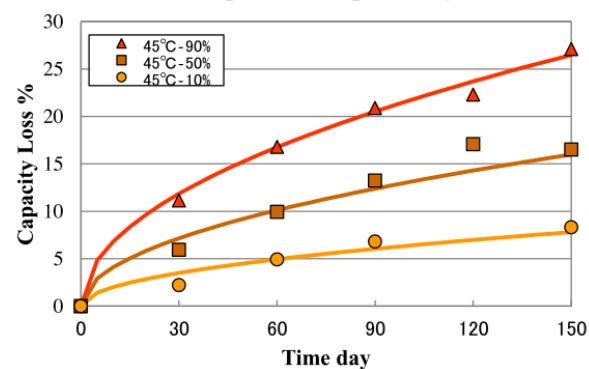
Accelerated EV battery degradation is a fear that holds people back from implementing V2X charging. The degradation of the common used EV battery type Li-ion are therefore investigated in this section.

The capacity degradation of a Li-ion battery is a function of the square root of time [13]. In addition, temperatures and the SOC of the battery effect the capacity losses as shown in Figure 2-7. The capacity losses are the most substantial when the battery is kept at a high environmental temperature and while having an high SOC.

The capacity loss of EV batteries due to high temperatures and high SOC is not taken into account in this thesis since the microgrid simulation period of two weeks is considered to have an insignificant effect on the battery capacity. Furthermore, the mentioned battery degradation is independent from the used charging strategy, e.g. uncontrolled charging or smart charging, and therefore not important to take into account.



(a) Temperature dependency



(b) SOC dependency

Figure 2-7: Li-ion battery capacity loss over time considering varying temperatures (a) and SOC's (b) [13].

The capacity loss of a Li-ion battery is also dependent on the number of charge cycles and the depth of discharge, see Figure 2-8. A higher depth of discharge results in a higher capacity loss when increasing the number of charge cycles. In practice this would mean that if an EV needs to charge once a week with 50 % discharge depth, a battery capacity of 10 % is lost after roughly twenty years. The battery capacity loss is therefore not a significant problem in regular charging behavior. However, when V2H is used, i.e. the EV is possibly charged and discharged multiple times a day, the capacity deterioration can be a relevant problem. A constraint is therefore implemented in the V2H charging strategy to prevent the charging and discharging of the EV battery too often, see Section 3-2-4.

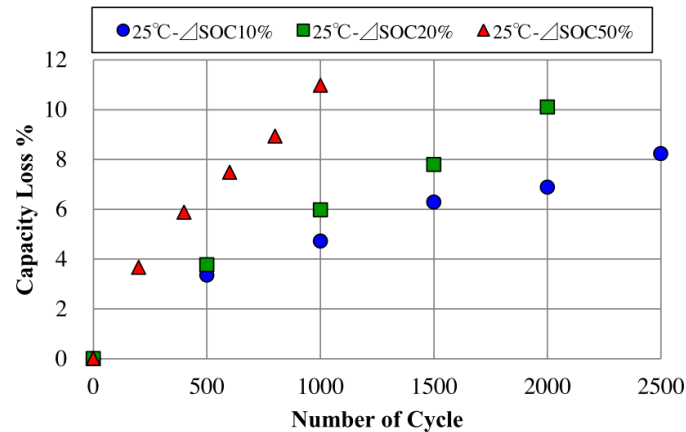


Figure 2-8: Li-ion battery capacity loss over number of charge cycles with varying depth-of-discharge [13].

2-2-4 Travel profile of electric vehicles

The travel behavior of EV owners is important to consider when modelling a microgrid as it depicts when the EVs are used for transportation and how much energy is needed to charge them. The travel behavior of EV owners is therefore investigated in this section. The yearly driven distances are discussed first after which the charging pole arrival and departure times are addressed.

Driven distances

Statistics Netherlands (CBS) has data of the yearly driven distances of cars, i.e. both combustion engine vehicles and EVs, in the Netherlands as shown in Figure 2-9 [8]. A spline interpolation is used find the mean yearly driven distance which is approximately 13 770 km. There is a large spread in the in driven distances as a car owner has different needs for the car, e.g. going to work or doing groceries. It is assumed that the reasons for which people drive cars do not change when people drive EVs. It is therefore assumed in this thesis that the current combustion engine vehicle driving behaviors also holds for EVs drivers.

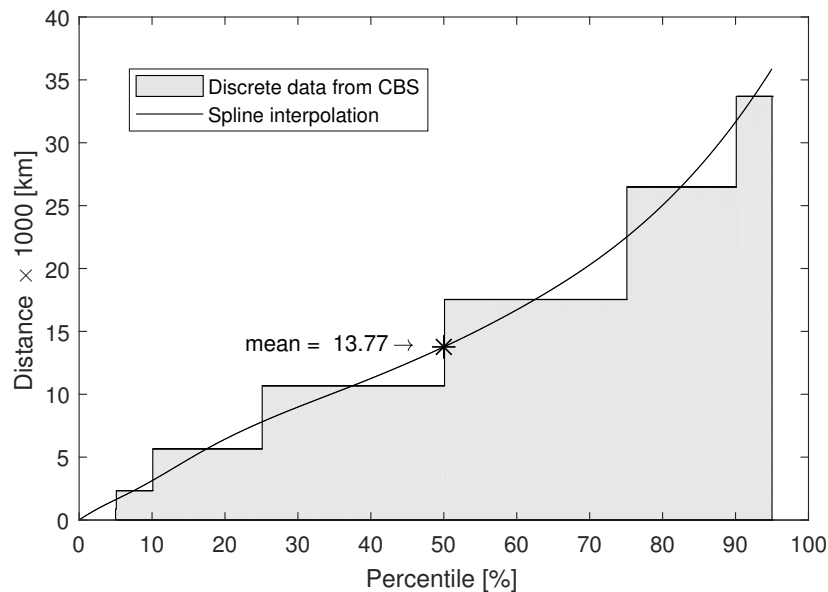


Figure 2-9: Yearly driven distances with cars in the Netherlands in 2017.

Arrival and departure times

ElaadNL provided data of twenty thousand charging sessions of electric vehicles between the year 2016 and 2019 of public EV charging stations in the Netherlands [28]. This data is used to retrieve charging pole arrival and departure times of EVs. All the charging sessions can be clustered into three groups namely, the charge-near-home, the park-to-charge, and the charge-near-work group [29]. This partitioning is shown in Figure 2-10 where the daily normalized arrival and departure times of the charging sessions are plotted. A data point below the diagonal indicates a charging session with an arrival before and departure after midnight at a charging pole.

The cluster groups are distinguished by the charge duration and by the arrival and departure time of the EVs at the charging pole. For instance, the charge-near-home group is characterized by arrivals at the evening and departures at the subsequent morning. Furthermore, seasonal and weekend differences in arrival and departure times were also identified. The EVs tend to arrive earlier at the charging pole in the spring and summer season compared to the autumn and winter season. In addition, EVs tend to arrive later at the charging poles in the weekends than during the week.

The mean connection time to the charging pole in the park-near-home cluster is roughly 13.5 hours of which only the first 3.5 hours are used to actually charge the EV using an uncontrolled charging strategy. This leaves 10 hours of idle connection time which indicates that there is more than enough possibility to charge the EV at later times using smart charging or V2H charging in view of cheaper electricity rates.

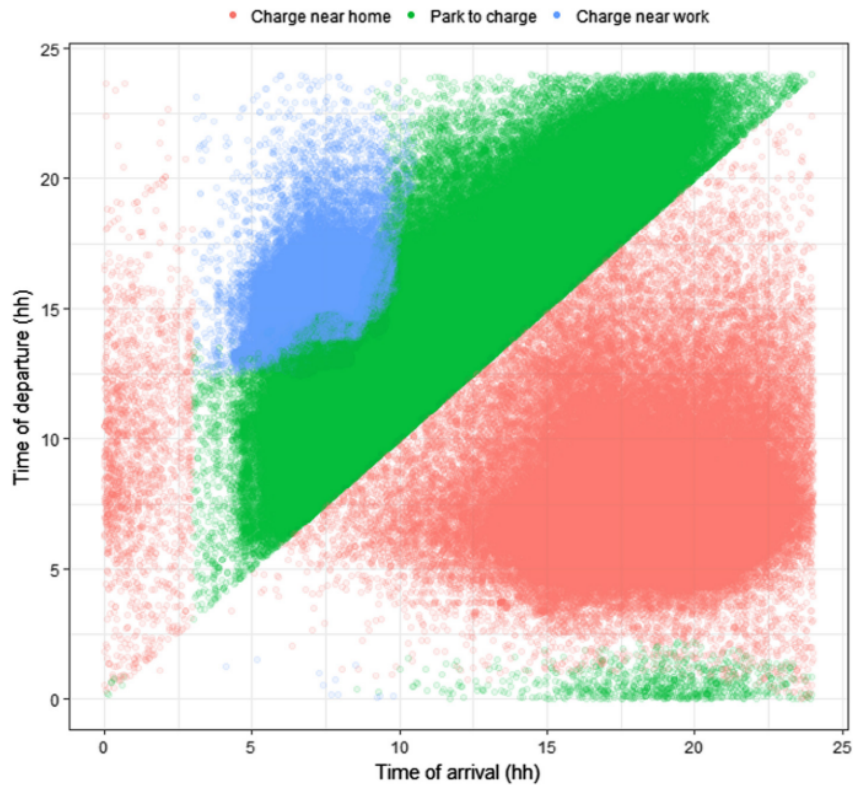


Figure 2-10: Clustered normalized charging pole arrival and departure times [29].

2-3 Photovoltaic generation

Sunlight can be converted into electricity by the use of PV panels without generating pollution. PV generation is therefore a popular and subsidized energy technology in the Netherlands.

Stedin provided generation data of a 65 m² roof with PV panels located in the Netherlands, see Figure 2-11. Disclosure of details regarding the PV generation data is kept to a minimum due to privacy reasons.

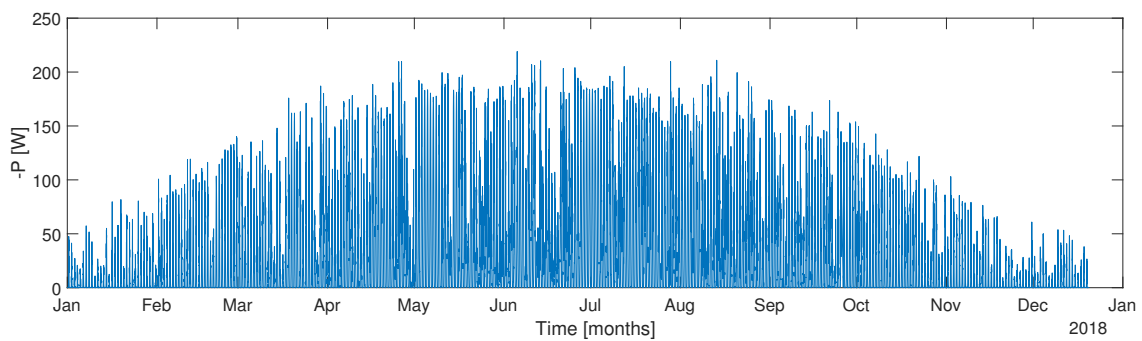


Figure 2-11: Production profile per PV Panel.

During the data analysis, a typical PV generation profile could be seen, see Figure 2-12 where the maximum, minimum, and median (i.e. middle value of an ordered set) generation profiles are shown. The generation starts in the morning after which the power increases until it has its maximum after noon. The power decreases thereafter and is zero at and end of the day. This profile repeats each day and coincides with the rising and setting of the sun. The power generation output depends on the time of the year. There is a higher power output during the summer season than the in the winter season. Occasional high frequent disturbances are observed in the PV generation profile are caused by the presence of clouds which reduce the PV generation. Since the disturbances, i.e. clouds, are highly local, the production profile is expected to be more smooth when using a larger and more erratic when using a smaller PV generation surface. Considering the standard sizing of a PV panel of $1\text{ m} \cdot 1.65\text{ m}$, the maximum power output per panel during the year is approximately 220 W.

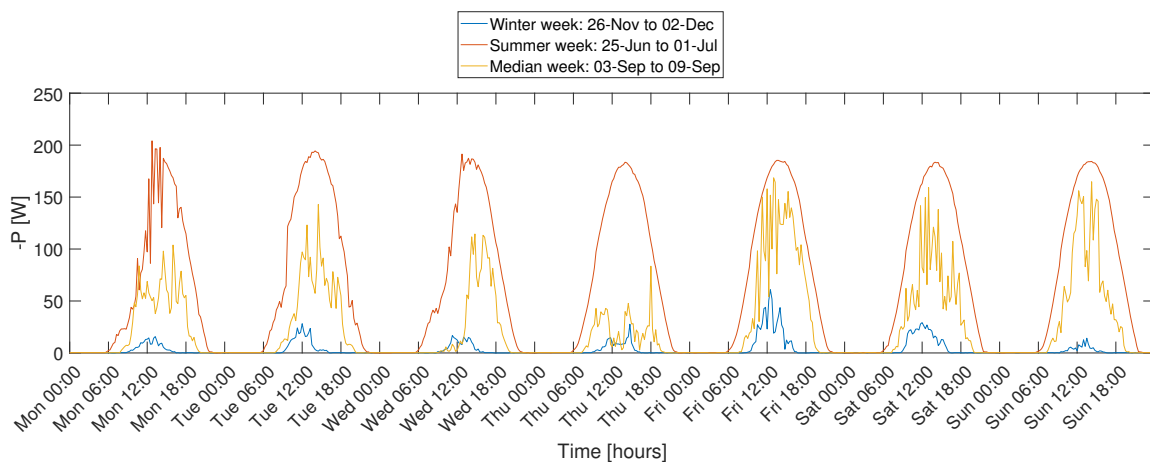


Figure 2-12: Maximum, median, and minimum production week per PV panel in 2018.

2-4 Household loads

The Dutch society of energy data exchange (NEDU) has published normalized aggregated electricity load profiles of consumers based on their connection size to the main grid [17]. Figure 2-13 shows the yearly power profile normalized to 1 kWh of energy usage with connection smaller or equal than three phase 25 A. Seasonal effects are clearly distinguished with higher electricity demands during the winter than during the summer season.

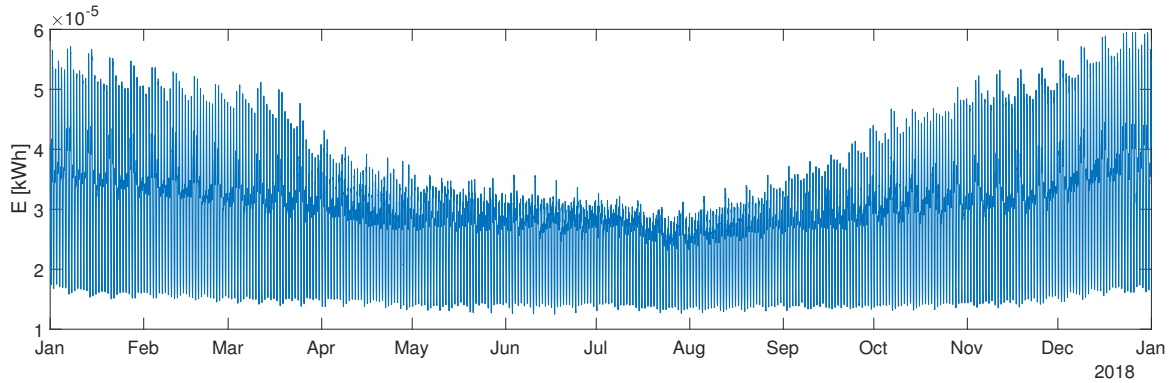


Figure 2-13: Household load profile 2018 ($\leq 3 \cdot 25$ A) with normalized electricity usage.

Figure 2-14 shows the weekly power profiles plotted over each other and the mean profile is also shown. The fact that the data depicts aggregated profiles should be kept in mind. Load profiles of single households would have much more sporadic power profiles with extrema which could largely differ from the shown data.

A daily pattern is observed after analyzing the mean profile which is described as follows. The lowest electricity demand is around 2:00 hrs., i.e. when most people are sleeping. In the early morning, the electricity usage quickly rises after which it remains roughly stable. This is attributed to people waking up and starting to use electrical appliances. There is a relatively small dip in demand between noon and 17:00 hrs., this dip is more profound in the weekends compared to the weekdays. Between 17:00 hrs. and 22:00 hrs., the largest demand of electricity occurs. This is due to people arriving home from work or school and starting to use appliances again. This peak demand is expected to grow in the future as explained in Section 1-1-1. Most people go to sleep after 22:00 hrs., the electricity demand decreases quickly in this period. The daily demand profile repeats itself thereafter.

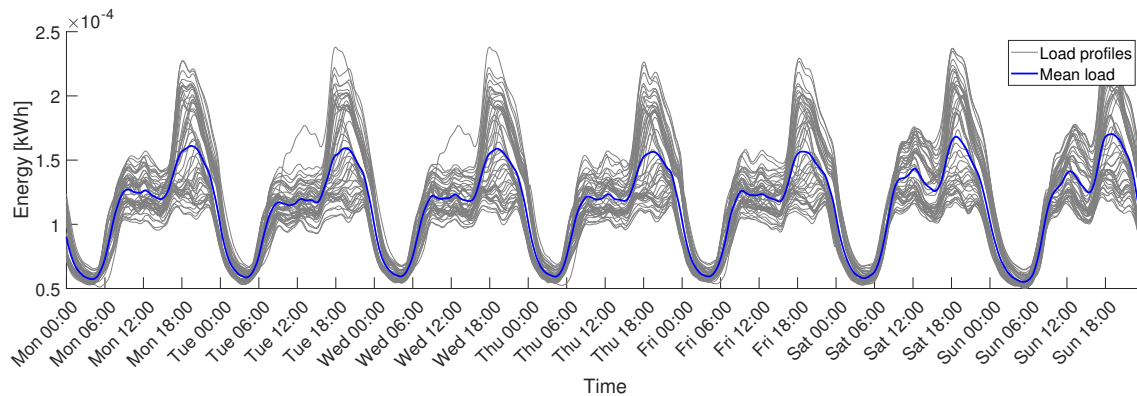


Figure 2-14: Weekly household load profiles 2018 ($\leq 3 \cdot 25$ A) normalized electricity usage.

Both the normalized electricity demand profiles and anonymised data of yearly electricity usage from Stedin clients are employed together for the microgrid simulations in this thesis.

2-5 Conclusions

This chapter introduced several topics related to microgrids which will provide a solid background for this thesis. In Section 2-1, the advantages and the related challenges for the use of microgrids were described. In addition, the hierarchical control structure of the microgrid was introduced and it was concluded that the tertiary control layer is best suited for implementing EV charging strategies. Thereafter, the variable electricity price and the costs for the DSO were presented as the economical household costs in a microgrid. The EV was discussed subsequently in Section 2-2 where a description was given of the advantages of EV adoption, different charging strategies (i.e. uncontrolled charging and V2X charging), battery degradation, and the travel profile of EV users. It was concluded that smart charging and V2H charging are most suited for this thesis to reduce the economical microgrid costs. Finally, the PV generation and the household load profiles were discussed in Section 2-3 and Section 2-4 respectively. The presented topics in this chapter are taken in to account through the development of both the microgrid model and the control algorithms which will be explained the subsequent chapter.

Microgrid modelling and control

This chapter presents which microgrid modelling methods and control frameworks are used in this thesis. The modelling of microgrid systems and electric vehicles (EVs) are shown first in Section 3-1 and 3-2. In Section 3-3, the reformulation of non-linear models is discussed through the use of the mixed logical dynamical (MLD) framework. Section 3-4 elaborates the developed simple rule-based control algorithm. A more sophisticated control strategy, i.e. model predictive control (MPC), is presented in Section 3-5 together with the scenario-based MPC algorithm. Finally, several scenario generation methods are introduced in Section 3-6.

3-1 Microgrid modelling

The microgrid is modeled as if all the distributed energy resources are connected on one phase line and reactive power is assumed to be non-existent to reduce complexity. The microgrid model will contain EVs, household loads, and photovoltaic (PV) panels. The EV model is presented in Section 3-2. However, no model is used to simulate the household loads and the PV generation as the data as presented in Section 2-4 and 2-3 is used for simulation. The following sections will present the most important microgrid system dynamics considered in this research, i.e. the power equilibrium and the economical costs.

3-1-1 Power equilibrium

The most fundamental constraint in microgrids is the power equilibrium, i.e. the demand and supply in the grid of electricity must be equal. Problems can occur such as frequency deviations, voltage drops, and outages if the power equilibrium is not maintained. In this research however, it is assumed that the electricity demand of the microgrid can always be fulfilled through the supply of the main grid. Likewise, the microgrid can always provide a surplus of electricity back to the main grid. The microgrid is therefore never in an isolated state. The power equilibrium is described as:

$$P^g(k) = \sum_{i=1}^{n_{EV}} P_i^{EV}(k) + P^{PV}(k) + P^{ah}(k),$$

with $P^g(k)$, $P^{EV}(k)$, $P^{PV}(k)$, and $P^{ah}(k)$ as the grid power, the EV charge power, the PV generation, and the aggregated household load respectively. The parameter n_{EV} denotes the total number of EVs in the microgrid.

3-1-2 Economical costs

As discussed in Section 2-1-3, the economical microgrid costs consist of costs due to the electricity supplier and due to the distributed system operator (DSO).

The microgrid costs due to the electricity supplier $C^{el}(k)$ is dependent on the electricity exchange with the main grid and is described by the following piece-wise affine model:

$$C^{el}(k) = \begin{cases} c^p(k)P^g(k) & \text{if } P^g(k) \geq 0 \\ c^s(k)P^g(k) & \text{if } P^g(k) < 0, \end{cases}$$

where $c^p(k)$ and $c^s(k)$ are respectively the current purchase and sale prices of electricity.

The microgrid DSO costs C^{DSO} are mainly dependent on the peak power demand to the grid in a period and is modeled as:

$$C^{DSO} = c^{DSO} \max(\{P^g(1), \dots, P^g(N_s)\}),$$

where N_s is the final time instant and c^{DSO} the DSO cost weight.

3-2 Electric vehicle modelling

The EV model is described in this section where several model aspects related to the charging of EVs are highlighted. The EV battery dynamics are presented first. The constraints due to the charge power limitation, range anxiety, and battery degradation are discussed thereafter. Finally, a description is given of how certain EV properties vary between each EV in the microgrid.

3-2-1 Battery dynamics

The EV battery state dynamics are dependent on what the EV is currently being used for, e.g. driving or charging. The battery state dynamics are therefore formulated as a piece-wise affine model as shown in Equation 3-1:

$$x(k+1) = \begin{cases} A := x(k) - E^{\text{dem}} & \text{if } \delta^c(k) = 1 \wedge \delta^c(k+1) = 0 \\ B := x(k) + T_s \eta P^{EV}(k) & \text{if } \delta^c(k) = 1 \wedge \delta^c(k+1) = 1 \\ C := x(k) & \text{if } (\delta^c(k) = 0 \wedge \delta^c(k+1) = 0) \dots \\ & \vee (\delta^c(k) = 0 \wedge \delta^c(k+1) = 1), \end{cases} \quad (3-1)$$

where $x(k)$ denotes the EV battery level at time instant k and the binary variable $\delta^c(k)$ indicates if the EV is connected to a charging pole. Three different EV states are distinguished: departure from charging pole, connected to charging pole, or not connected to charging pole, denoted respectively by parts A, B, and C.

When the EV is used for driving, it will gradually deplete the battery in reality. However, to reduce model complexity, the energy depletion is modeled as an instantaneous energy loss E^{dem} during charging pole departure, i.e. part A in Equation 3-1. The battery level remains equal after EV departure, i.e. part C. When the EV is connected, i.e. part B, the battery level is dependent on the power exchange P^{EV} with the charging pole while taking into account the power conversion efficiency η as discussed in Section 2-2-2. The converted power is multiplied with the sampling time T_s to obtain the amount of exchanged energy. The power conversion efficiency is dependent on the EV charge power as follows:

$$\eta = \begin{cases} \eta^c & \text{if } P^{\text{EV}}(k) \geq 0 \\ \frac{1}{\eta^d} & \text{if } P^{\text{EV}}(k) < 0, \end{cases} \quad (3-2)$$

where η^c and η^d denote the charge and discharge efficiency respectively. The battery dynamics are implemented separately for each EV in the microgrid since each EV has different characteristics as discussed in Section 3-2-5.

3-2-2 Charge power limitation

As explained in Section 2-2-2, the maximum EV charge power is modeled to be dependable on the battery level from a state of charge (SOC) of 87.5 % and higher. This dependency is approximated through a linear function in a piece-wise affine model for the maximum EV charge power:

$$\bar{P}^{\text{EV}}(k) = \begin{cases} \bar{P}^{\text{EV}} & \text{if } \text{SOC} < 87.5\% \\ a^{\text{lin}} \frac{x(k)}{E^{\text{cap}}} + b^{\text{lin}} & \text{if } \text{SOC} \geq 87.5\%, \end{cases} \quad (3-3)$$

where $\bar{\cdot}$ represents the maximum of the considered variable and $a^{\text{lin}}, b^{\text{lin}}$ are parameters of the linear approximation.

The EV power limitation constraint is then described as follows:

$$\delta^c(k) \underline{P}^{\text{EV}} \leq P^{\text{EV}}(k) \leq \delta^c(k) \bar{P}^{\text{EV}}, \quad (3-4)$$

where $\underline{\cdot}$ represents the minimum of the considered variable. Note that \bar{P}^{EV} does not depend on k as $x(k)$ in Equation 3-3 is known when the controller determines an optimal $P^{\text{EV}}(k)$. The $\delta^c(k)$ multiplication in Equation 3-4 is to ensure that the charge power is zero when the EV is not connected to the charging pole.

3-2-3 Range anxiety

Ensuring that the EV user has a full battery at charging pole departure will help the smart charging and vehicle-to-home (V2H) charging participation rates due to range anxiety as explained in Section 2-2-2 and is presented through the following equation:

$$x(k) = \bar{x} \quad \text{if} \quad \delta^c(k) = 1 \wedge \delta^c(k+1) = 0.$$

Furthermore, each EV has a minimum SOC battery level assigned to it which is the minimum amount of energy that the EV should always have while connected to a charging pole. Through this constraint, the EV user is still able to use the EV for incidental trips made earlier than the known EV departure time, which mitigates the potential range anxiety further.

3-2-4 Battery degradation constraint

The EV battery capacity degradation is dependent on the number of charge cycles as explained in Section 2-2-3. The smart charging strategy only spreads and shifts the needed EV energy compared to uncontrolled charging. It is therefore expected that smart charging does not impose an increased battery degradation compared to uncontrolled charging. However, as the V2H charging strategy allows a bi-directional power flow, the number of charge cycles using V2H charging can be significantly more compared to the smart charging strategy. To mitigate this increased battery degradation, a constraint is implemented for the V2H charging strategy which ensures that switching between charging and discharging the EV is only allowed after a time interval of 30 minutes.

3-2-5 Varying properties

Certain EV related properties (i.e. charging pole arrival and departure times, the battery capacity, and the daily energy demand) are varied between each EV such that a better reflection of reality is achieved in the microgrid model. The varying properties are implemented through creating distributions of the EV features and using the roulette wheel method, as explained in Section 3-6-1, to assign different property values to each EV in the microgrid.

A normal distribution of the EV battery capacity is created using the mean in Table 4-1 and a standard deviation of $\sigma = 10$ kWh. Furthermore, the charging pole arrival and departure times of EVs are taken from the charge-near-home group as presented in Section 2-2-4. A distribution of the daily energy demand of EVs is developed from the distribution of yearly driven distances of cars and through using the fact that the average EV drives 5 km/kWh [1, 8]. Each EV in the microgrid is assumed to have the same driving efficiency as it only has a minor effect on the daily EV energy demand.

3-3 Mixed logical dynamical framework

An MPC algorithm is used in this thesis to implement smart charging and V2H charging, see Section 3-5. The algorithm solves an optimal control problem to find the control action for the

following time instant in the simulation. Implementation in on-line control becomes therefore intractable when the MPC algorithm takes too much time to solve the programming problem. It is therefore desired to keep the microgrid model complexity as low as possible. The current microgrid model is non-linear due to e.g. piece-wise affine battery dynamics. Therefore, an MLD framework is used to reformulate the model into an efficient solvable mixed integer linear programming (MILP) problem [25].

The MLD framework introduces auxiliary variables that are either binary, e.g. $\delta(k)$, or continuous, e.g. $z(k)$ [3]. The auxiliary variables are related to other continuous variables, e.g. $f(k)$, through implementing constraints as shown Equation 3-5:

$$f(k) \geq 0 \iff \delta(k) = 1 \quad \text{is true iff} \quad \begin{cases} -\underline{f}\delta(k) \leq f(k) - \underline{f} \\ -(\underline{f} + \epsilon)\delta(k) \leq -f(k) - \epsilon \end{cases} \quad (3-5a)$$

$$f(k) \leq 0 \iff \delta(k) = 1 \quad \text{is true iff} \quad \begin{cases} f(k) \leq \bar{f}(1 - \delta(k)) \\ -f(k) \leq -\epsilon - (\underline{f} - \epsilon)\delta(k) \end{cases} \quad (3-5b)$$

$$z(k) = f(k)\delta(k) \quad \text{is equivalent to} \quad \begin{cases} z(k) \leq \bar{f}\delta(k) \\ -z(k) \leq -\underline{f}\delta(k) \\ z(k) \leq f(k) - \underline{f}(1 - \delta(k)) \\ -z(k) \leq -f(k) + \bar{f}(1 - \delta(k)), \end{cases} \quad (3-5c)$$

where the constant ϵ denotes a small number, typically the machine precision.

The reformulation of the battery state dynamics using the MLD framework is briefly shown here to illustrate the process. See Appendix A for the full reformulation of the battery state dynamics. The auxiliary variables:

$$\delta^{\text{EV}}(k) = 1 \iff P^{\text{EV}}(k) \geq 0 \quad z^{\text{EV}}(k) = \delta^{\text{EV}}(k)P^{\text{EV}}(k),$$

are introduced together with the related constraints as shown in Equation 3-5. Implementing the introduced auxiliary variables in Equation 3-1 results in the following piece-wise affine equation:

$$x(k+1) = \begin{cases} A := x(k) - E^{\text{dem}} & \text{if } \delta^{\text{c}}(k) = 1 \wedge \delta^{\text{c}}(k+1) = 0 \\ B := x(k) + T_s(\eta^{\text{c}} - \frac{1}{\eta^{\text{d}}})z^{\text{EV}}(k) + \frac{T_s}{\eta^{\text{d}}}P^{\text{EV}}(k) & \text{if } \delta^{\text{c}}(k) = 1 \wedge \delta^{\text{c}}(k+1) = 1 \\ C := x(k) & \text{if } \delta^{\text{c}}(k) = 0 \wedge \delta^{\text{c}}(k+1) = 0, \end{cases} \quad (3-6)$$

where part B of the model is made linear in its parameters while taking into account a correct power conversion efficiency implementation. Finally, through using the EV connected indicators from the model battery parts, the model is rewritten as a single MILP equation:

$$\begin{aligned} x(k+1) &= \delta^{\text{c}}(k) \left(\delta^{\text{c}}(k+1) B + (1 - \delta^{\text{c}}(k+1)) A \right) + (1 - \delta^{\text{c}}(k)) C \\ &= \delta^{\text{c}}(k) \delta^{\text{c}}(k+1) \left(\left(\eta^{\text{c}} - \frac{1}{\eta^{\text{d}}} \right) T_s z^{\text{EV}}(k) + \frac{T_s}{\eta^{\text{d}}} P^{\text{EV}}(k) + E^{\text{dem}} \right) - \\ &\quad \delta^{\text{c}}(k) E^{\text{dem}} + x(k). \end{aligned} \quad (3-7)$$

The reformulation process is similar for the other presented piece-wise affine equations.

3-4 Rule-based control

Rule-based control is used in this research to implement the charging strategies, i.e. uncontrolled charging, smart charging, and V2H charging, as it is straightforward to implement. Another advantage is that the control algorithm can incorporate if-then statements, e.g. charge with maximum power if an EV arrives at the charging pole. If-then statements are a natural and structural way to approach the microgrid control problem.

Figure 3-1 shows a decision tree which represents the developed rule-based control algorithm. The decision tree is used at each time instant during the microgrid simulation and decides for each charging pole what the EV charge power should be. The rule-based control algorithm makes several decisions, depending on the implemented control algorithm, to determine the EV charging power.

Firstly, the rule-based control algorithm checks if an EV is connected to the charging pole, if this is not the case, no power is given to the charging pole. When an EV is connected to the charging pole, it can only be possibly charged if the EV battery is not already full. When the EV battery is lower than 100 % SOC, the rule-based controller checks the implemented charging strategy. If uncontrolled charging is considered, the EV will be charged using maximum power, denoted in Figure 3-1 as P_{\max}^{EV} instead of \bar{P}^{EV} , as defined in Equation 3-4. If either smart charging or V2H charging is considered, the minimum power that the EV needs to receive for all coming future time instants to have a full battery before its departure from the charging pole is considered. If the needed power is higher or equal to \bar{P}^{EV} , the EV will be charged with maximum power to have a full battery at departure. When the needed power for a full battery is lower than \bar{P}^{EV} , the current electricity price is considered. The electricity price is considered high or low based on the current time in the simulation using generalizations made from Figure 2-4, e.g. the price is low between 22:00 hrs. and 7:00 hrs. If the current electricity price is low, the EV is charged with the minimum value between the \bar{P}^{EV} and the peak power charge margin, denoted as $P_{\text{peak_margin}}^{\text{EV}}$. The peak power charge margin is the amount of power that all connected EVs can charge with while not increasing the historical aggregated peak power demand to the main grid. The margin is taken into account to confine the DSO costs as much as possible. If the current electricity price is high while the smart charging strategy is considered, the EV will not be charged. However, if the current electricity price is high while a V2H charging strategy is considered, the EV is allowed to discharge with the maximum value between the minimum charge power $\underline{P}^{\text{EV}}$, depicted as P_{\min}^{EV} in Figure 3-1, and the zero power margin $P_{\text{zero_margin}}^{\text{EV}}$. The zero power margin is the amount of discharge power that all connected EVs could discharge collectively to provide the households in the microgrid with power without selling electricity back to the main grid. This margin is implemented since the selling price of electricity is much lower than the buying price which makes it less profitable to sell electricity back to the grid, see Section 2-1-3.

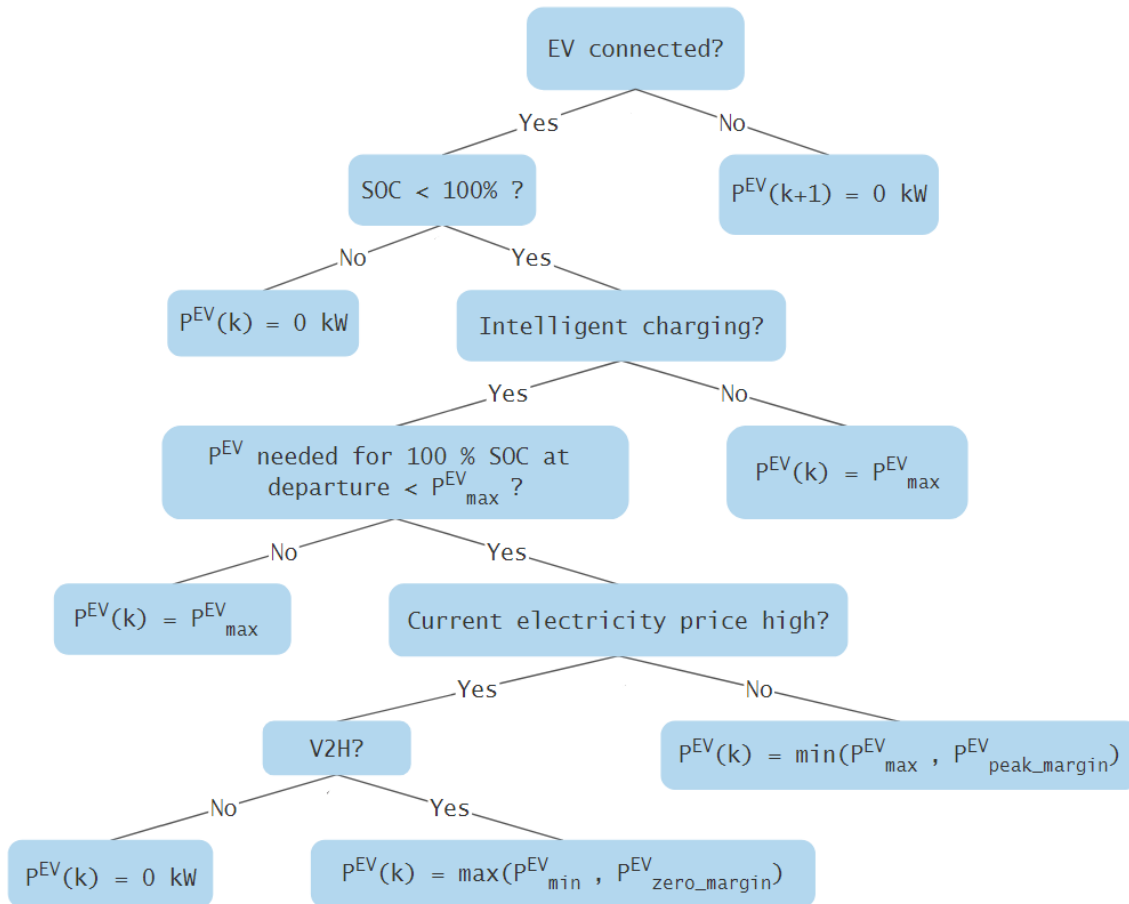


Figure 3-1: Rule-based control decision tree for uncontrolled charging, smart charging, and V2H charging.

3-5 Model predictive control

This section presents the MPC framework. First, a general description is given of the control algorithm such that a basic understanding is developed. Thereafter, the MPC implementation in microgrids is considered.

3-5-1 General description

The MPC framework makes explicit use of a model to compute a control signal through minimizing a possibly constrained cost function while simulating future states in a receding horizon fashion. In general, the aim is that a future output on the considered horizon should follow a determined reference signal or be driven towards an equilibrium point while penalizing the needed control effort.

MPC algorithms are able to deal with different control challenges such as optimal, stochastic, dead time, and multi-variable control [6]. Nevertheless, it is conceptually easy to understand.

Various MPC algorithms only differ amongst themselves in the model used to represent the process, the disturbances which are present in the model, and the cost function to be minimized.

A drawback of MPC strategies is that implementation in on-line control results in a higher amount of computational complexity compared to implementing e.g. classical proportional–integral–derivative or rule-based controllers, even more so when taking into account system constraints. In addition, the performance of MPC depends greatly on the quality of the used model.

A general mathematical foundation of MPC is given below [6, 15]. Consider a linear time-invariant system of the discrete-time type:

$$\begin{aligned} x(k+1) &= Ax(k) + Bu(k) \\ y(k) &= Cx(k), \end{aligned} \quad (3-8)$$

where A , B , and C are the system matrices and the variables $x(k)$, $u(k)$ and $y(k)$ denote respectively the state, control input, and measured output at sampling instant k . MPC approaches the following optimal open-loop control problem at each time instant k :

$$\min_{\mathbf{u}} J(x(k), \mathbf{u}) \quad (3-9a)$$

$$\text{subject to } x(k+i+1|k) = Ax(k+i|k) + Bu(k+i|k) \quad (3-9b)$$

$$Hx(k+i+1|k) \leq h \quad (3-9c)$$

$$Du(k+i|k) \leq d \quad (3-9d)$$

$$i = 0, 1, \dots, N_h - 1 \quad (3-9e)$$

$$x(k|k) = x(k), \quad (3-9f)$$

where N_h is the prediction horizon and $k+i|k$ denotes the predicted value of a variable at a future time instant $k+i$, based on the knowledge of the system at time instant k . The matrices H and D are constraints on the states and input respectively, with h and d denoting the corresponding constraint values for the state and input constraints. Equation 3-9f ensures that the initial conditions of the optimal control problem remain unchanged. The cost function $J(x(k), \mathbf{u})$ is commonly chosen as a regularization cost for driving the state and input to zero:

$$J(x(k), \mathbf{u}) = \sum_{i=0}^{N_h-1} (x^\top(k+i|k)Q_x x(k+i|k) + u^\top(k+i|k)R_u u(k+i|i)), \quad (3-10)$$

where $\mathbf{u} := \{u(k|k), u(k+1|k), \dots, u(k+N_h-1|k)\}$ is a sequence of control inputs, and the matrices $Q_x \geq 0$ and $R_u > 0$ are weight matrices. Equation 3-9 is a convex quadratic programming problem which can be solved efficiently.

Only the first element of the open-loop optimal control input is applied to the system. Subsequently, the optimization is solved again for the next time instant, this process continuous reiteratively in a receding-horizon manner.

3-5-2 Microgrid implementation

A few modifications have to be made on the general MPC framework presented in the previous section to be able to use the algorithm in a microgrid system [25]. The MPC objective function, i.e. the cost function, as shown in Equation 3-10, is not suitable to implement in microgrid control. Therefore, a description of a suitable MPC cost function is discussed first.

The aim of the MPC algorithm is to determine a value for the microgrid system input, i.e. the EV charge power flow $P^{EV}(k)$, while keeping the economical microgrid costs as low as possible, i.e. the electricity price and the DSO costs as explained in Section 2-1-3. The economical costs are therefore part of the MPC cost function. Furthermore, the implementation of the full EV battery at charging pole departure constraint, as described in Section 3-2-3, can cause infeasibility problems in the optimal control problem. The constraint is therefore reformulated into a soft constraint and also implemented in the cost function. Moreover, a high penalty is implemented in the cost function when the SOC of the EV battery drops below a certain threshold value such that the EV battery is never completely empty, see Section 3-2-3. Although the constraint is implemented through the cost function, it is not considered to have a fundamental effect on the control action. In summary, the main cost drivers in the objective function are the economical costs and the full EV battery at charging pole departure costs.

The different microgrid costs in the objective function are weighted such that appropriate priorities are given to reducing the economical microgrid costs and filling up the EV battery for charging pole departure. The objective function weights remain the same in each simulation.

Some variables in the microgrid are difficult to model as they are subject to uncertainty, i.e. the household loads, the electricity price, and the PV generation. Therefore, two MPC cases are considered, namely the perfect information and the certainty equivalent case. The perfect information case is able to perfectly forecast the uncertain variables, i.e. there is no uncertainty. This case will give the best possible control performance. The certainty equivalent case is more realistic as it uses a persistence forecast model to predict future values of an uncertain variable. The persistence forecast model has a simple assumption on the uncertain variable as it assumes that future values will be the equal to the latest measurements, e.g. the PV generation of tomorrow is equal to that of today, see Equation 3-11:

$$P^{PV}(k+1|k) = P^{PV}(k+1-T|k), \quad (3-11)$$

where the variable T depicts a time shift. The time shift is set to one day backwards for the PV generation. However, the time shift for the household loads and the electricity price is chosen as one week backwards as the variables show a stronger weekly cyclic behavior, see Section 2-1-3.

The open-loop control problem of the microgrid MPC implementation is posed as a MILP problem due to the MLD framework presented in Section 3-3 which ensures efficient solving of the control problem.

3-5-3 Scenario-based

A disadvantage of the MPC framework, described in the previous section, is that it does not take into account uncertainty as only one forecast of uncertain variables, i.e. the household loads, the electricity price, and the PV generation, is assumed to occur. However, it is likely that the forecast of the uncertain variable deviates from the true measurements, e.g. tomorrow's weather can be sunnier or cloudier than expected which affects the PV generation. The scenario-based MPC is therefore introduced as control algorithm. The scenario-based MPC algorithm is similar to the regular MPC, but in addition, it can take into account multiple forecasts, i.e. scenarios, of uncertain variables and generate a control action that is optimized for all scenarios [26, 30]. It is therefore expected that the scenario-based MPC algorithm can outperform the MPC certainty equivalent case.

The number of needed scenarios is an important parameter in the scenario-based MPC algorithm. A high number of implemented scenarios will ensure that the uncertainty of variables is represented well in the open-loop control problem. However, a high number of scenarios will also result in high computational complexity and could generate a conservative control action. In addition, a high representation of the uncertainty is only useful when the implemented scenarios form a good approximation of the real uncertainty which is difficult to achieve. The number of implemented scenarios is therefore a trade-off between depicting the uncertainty well and generating a conservative control action with high computational complexity.

3-6 Scenario generation

As discussed in the previous section, the scenario-based MPC algorithm can possibly give improved performance compared to the MPC algorithm. The scenario-based MPC algorithm achieves this through taking into account multiple scenarios for each uncertain variable, i.e. the household loads, the electricity price, and the PV generation, such that the optimal control input is also optimized for uncertainty. However, there is only one good point forecast available, i.e. the persistence forecast model. In this section, six different methods are presented, which are used to generate additional scenarios such that they can be implemented in the scenario-based MPC. The generated scenarios through these methods are always implemented in addition to the single point forecast scenario generated from the persistence forecast model. The five scenario generation methods which use the historical forecast errors are highlighted first after which the matching profile scenario generation method is presented.

3-6-1 Historical forecast error methods

The historical forecast scenario generation methods use information of the historical forecast error to generate new scenarios from an available point forecast. In general, the historical forecast errors are collected into an error distribution in the form of an histogram. Thereafter, new scenarios are generated through sampling from the error distribution using the roulette wheel method and adding them to the point forecast. This scenario generation process and its variants are explained in more detail in this section.

Error collection

The most straightforward period to collect historical forecast errors from is the past year. When the yearly forecast error distribution is randomly sampled and added to the point forecast, the assumption is made that the uncertain variable has stationary stochastic properties, i.e. the statistical properties of the forecast error do not change over time. This assumption can be inaccurate, certainly in microgrid context where uncertain variables are often dependent on many factors e.g. the hour of the day or season in the year. The yearly forecast error collection is therefore used as a performance benchmark in the comparison with other scenario generation methods.

A different approach is to collect only the recent forecast errors, i.e. of the past 24 hours. In this way, short temporal stochastic behavior of the uncertain variable is incorporated through an adapting error distribution which is updated after each time instant. A disadvantage of this method is that it does not represent longer temporal stochastic behavior of uncertain variables very well as the size of the forecast error distribution is limited.

When the temporal stochastic properties are known of the uncertain variable, forecast error collection can be done while grouping the errors in these temporal characteristics. For instance, the PV generation has seasonal and hourly trends, e.g. more generation during the summer than in the winter and more generation during midday than early in the morning. The historical PV generation forecast error can therefore be grouped seasonally and hourly. The grouping creates several error distributions which are sampled when the related season and hour is forecasted in the simulation.

To summarize, three forecast error collection periods are used to implement the historical forecast error scenario generation methods: the past year, the past day, and hourly using seasonal data.

Roulette wheel method

When the forecast error distributions are obtained, they are sampled using the roulette wheel method to add the errors to the available point forecast to generate new scenarios. The roulette wheel method enables to random sample a histogram while taking the probability of those samples into account [20]. To implement the roulette wheel method, one first divides the collected forecast errors into a number of chosen intervals i.e. bins or levels, such that a histogram is obtained, see Figure 3-2. Probabilities of the bins are then assigned to each bin such that the total surface of the histogram has probability one. This is achieved through normalizing the frequency of samples in each bin to the total number of samples in the error distribution. The bins are subsequently stacked such that a binned zero to one probability is presented, see Figure 3-3. Next, one can draw a number from a standard uniform distribution which corresponds to one of the stacked bins from which a sample is drawn.

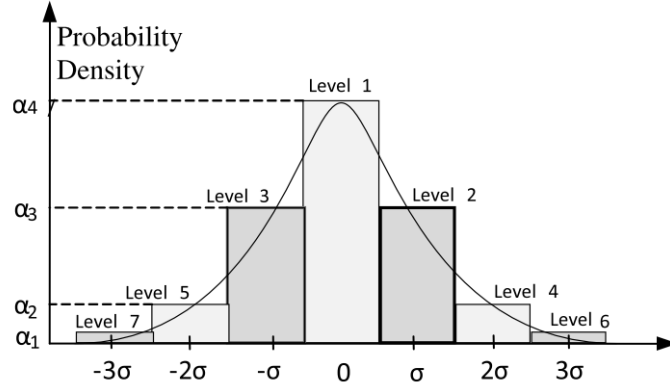


Figure 3-2: Normalized binned histogram with probability levels α_i [20].

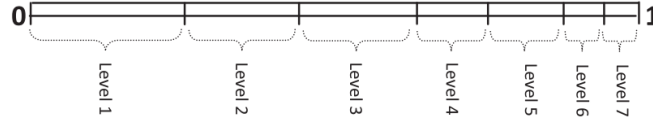


Figure 3-3: Cumulatively stacked probability bins [20].

Error addition

The construction of scenarios occurs by adding the sampled error from the forecast error distribution to the point forecast. In this research, two methods of error addition are considered for the construction of n_{sc} scenarios. The most straightforward method is to add a variable error at each time instant of the point forecast as shown in the example:

$$\begin{aligned}
 P_{scen,i}^{PV}(k+j|k) &= P_{pf}^{PV}(k+j|k) + e(k+j|k) \\
 j &= 0, 1, \dots, N_h - 1 \\
 i &= 2, 3, \dots, n_{sc},
 \end{aligned} \tag{3-12}$$

where the variables $P_{scen,i}^{PV}$, P_{pf}^{PV} , and e are respectively the i^{th} constructed PV generation scenario, the PV generation point forecast, and the sampled error. Note that the scenario index i starts at two as the first scenario implemented in the scenario-based MPC is the point forecast itself.

An advantage of adding a variable error to the point forecast is that the error distribution is sampled $n_{sc}N_h$ times in each time instant, i.e. a lot of uncertainty data is implemented in the scenarios. Adding a variable error method creates scenarios which all have different profiles from each other.

The second method adds a constant error to the whole point forecast as shown in the following example:

$$\begin{aligned}
P_{\text{scen},i}^{\text{PV}}(k+j|k) &= P_{\text{pf}}^{\text{PV}}(k+j|k) + e(k|k) \\
j &= 0, 1, \dots, N_h - 1 \\
i &= 2, 3, \dots, n_{\text{sc}}.
\end{aligned} \tag{3-13}$$

Scenarios constructed with constant errors are upwards or downwards shifted versions of the point forecast profile, i.e. the scenarios from a band around the point forecast. The scenario-based MPC algorithm optimizes for those scenarios and the optimal control solution might also give reasonable performance for scenarios which are not generated but lie inside the outer scenario bands around the point forecast. In other words, the scenario-based MPC algorithm might give equal performance while using a lower number of scenarios as the controller might take into account not constructed scenarios situated in between the generated scenarios.

A possible disadvantage of constant error addition is that the optimal control solution is too conservative, e.g. an outlier scenario increases the scenario band such that a lot of extra implicit scenarios are also taken into account. In addition, the error distribution is only sampled n_{sc} times in each time instant, this number might be too low for an adequate representation of the error distribution in the generated scenarios. Furthermore, the constant error addition creates scenarios that all have the same profile as the point forecast while the realization of the uncertain variable is likely to have a different profile.

To summarize, three periods of error collections are discussed from which are sampled and added to the point forecast either as a variable or as a constant. This means that there are $3 \cdot 2 = 6$ historical scenario generation methods which can be used for the scenario-based MPC algorithm. However, the scenario profile difference between adding the error as a variable or as a constant using the hourly seasonal error collection period is small as the error distribution is sampled at least each hour. Therefore, the hourly seasonal error collection period is only implemented using the constant error addition. This results in a total of five historical scenario generation methods:

- Yearly error variable
- Yearly error constant
- Daily error variable
- Daily error constant
- Seasonal hourly error

The names of the mentioned scenario generation methods indicate the error collection period and how the error is added to the point forecast, e.g. the yearly error constant scenario generation method collects the error in a yearly period and adds it as a constant to the point forecast.

3-6-2 Matching profile method

The matching profile scenario generation method considers the profile of the uncertain variables of the past six hours and picks similar historical profiles as new generated scenarios.

The method is different from the historical scenario generation methods as the generated scenarios are not based on the persistence forecast model.

The method takes the profile of an uncertain variable of the past six hours and compares it with all past measurements in the year using the root mean square error technique as illustrated in the example below:

$$\text{root mean square error} = \sqrt{\left(\mathbf{P}^{\text{PV}}(k) - \mathbf{P}^{\text{PV}}(k - T)\right)^2},$$

where $\mathbf{P}^{\text{PV}}(k)$ is a vector of PV generation measurements of the past six hours up until the current time instant k and $\mathbf{P}^{\text{PV}}(k - T)$ is a vector vector with the same length as $\mathbf{P}^{\text{PV}}(k)$ but shifted a period $T > 6$ hours backwards in historic measurements. The root mean square error is calculated repeatedly while increasing T until the all historical measurements are compared. The historical profiles are subsequently ordered based on the value of the root mean square error and the best matches, i.e. profiles with lowest root mean square errors, are picked as scenarios.

An advantage of the matching profile method is that the generated scenarios have diverse profiles. However, temporal uncertainty information of the uncertain variable is completely disregarded as the scenario generation is purely based on matching the profile of past measurements.

The profile of the uncertain variable is analyzed only for the past six hours such that there is a balance between not taking into account enough information from the recent measurements, i.e. analyzing a too short time period, and finding less good profile matches, i.e. analyzing a too long time period.

3-7 Conclusions

This chapter highlighted the microgrid modelling methods and control methodologies used to implement and simulate uncontrolled charging, smart charging, and V2H charging. Microgrid modelling was discussed in Section 3-1 where the power equilibrium constraint and the economical costs were elaborated. The modelling of EVs was discussed thereafter in Section 3-2 where the battery dynamics were considered first after which several EV constraints were elaborated regarding the charge power limitation, range anxiety, and the battery degradation. Some model equations were posed as piece-wise affine equations which made the implementation of an MPC algorithm in on-line optimization inefficient as the optimal control problem was non-linear. The MLD framework was therefore introduced in Section 3-3 to reformulate the model equations such that a MILP problem was obtained, which can be solved efficiently. Furthermore, the rule-based control algorithm is introduced in Section 3-4 where its operation is explained through a decision tree. The more sophisticated control method MPC, presented in Section 3-5, allows to take into account future system states. First a general description of MPC is given after which adaptations are discussed regarding implementation in microgrid context. In addition, the implementation of a certainty equivalent and a perfect information MPC case are discussed thereafter. The scenario-based MPC algorithm is presented at the end of section 3-5 which allows to take into account multiple forecasts of uncertain variables. Finally in Section 3-6, six scenario generation methods are discussed:

- Yearly error variable
- Yearly error constant
- Daily error variable
- Daily error constant
- Seasonal hourly error
- Matching profile

The labeling of the scenario methods indicate the way the method constructs scenarios, e.g. the yearly error constant method collects the forecast error of the whole year and adds it as a constant to the persistence forecast model. The scenario generation methods are used together with the scenario-based MPC to implement microgrid control. The control algorithms and microgrid models discussed in this chapter are used to simulate the EV charging strategies as shown in the following chapter.

Simulation and results

This chapter presents the results of simulating two case studies through incorporating the microgrid models and control algorithms as discussed in the previous chapter. The New Orleans building is introduced as basis for the microgrid case studies in Section 4-1. Thereafter in Section 4-2, the first case study is presented which considers the primary research goal to find out which charging strategy, i.e. uncontrolled charging, smart charging, or vehicle-to-home (V2H) charging is the most effective in reducing the economical household costs. This is achieved through simulating the charging strategies using a rule-based controller and model predictive control (MPC) algorithm and comparing the results. Further research is done through the second case study, see Section 4-3, to investigate whether the total microgrid costs, using smart charging, can be reduced further by taking into account the uncertainty of the electricity price, the household loads, and the photovoltaic (PV) generation. This is achieved through using a scenario-based MPC algorithm and comparing six scenario generation methods while varying the number of implemented scenarios.

4-1 Case study introduction

The New Orleans building in Rotterdam is chosen as microgrid case study since it has several microgrid friendly characteristics, see Figure 4-1. First of all, with an height of 158 m, the building is the tallest residential complex building in the Netherlands which contains 235 apartments, i.e. households. Furthermore, right next to the building, there is an indoor parking lot with room for 268 cars. Moreover, the roof of the car parking has 672m² of unused area which could be used for PV generation. The high number of households, the car park availability, and the possibility of PV generation makes the building a good candidate for employment of smart charging and V2H charging strategies.

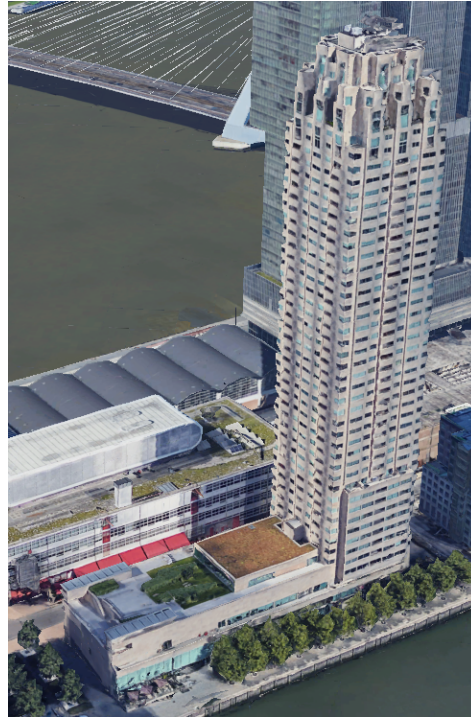


Figure 4-1: 3D model of the New Orleans building in Rotterdam [12].

A higher electric vehicle (EV) adoption will increase the potential economical benefits for the microgrid and is therefore interesting to consider. The microgrid case study is therefore viewed in the future year of 2040 as it is expected that during that time EV adoption will be much higher than today. Relevant data of the year 2040 is extracted from Table 4-1 and is translated to the New Orleans building. Through this method it is deduced that the microgrid will have 106 EVs, a 1.07 scaled household electricity demand compared to the demand of today, and a mean EV battery capacity of 90 kWh in the year 2040. Furthermore, the PV generation and the electricity prices from which data is available are used to simulate the microgrid in year 2040 as future developments of these variable are uncertain.

Table 4-1: Expected EV and household development in the Netherlands assuming a fast paced technology development [1].

| | 2015 | 2020 | 2030 | 2040 | 2050 |
|--|--------|--------|--------|--------|--------|
| Total number of EVs [$\cdot 1000$] | 8 | 50 | 1,484 | 3,831 | 5,224 |
| Total number of cars (including EVs) [$\cdot 1000$] | 7,977 | 8,321 | 7,420 | 6,384 | 5,224 |
| Total number of households [$\cdot 1000$] | 16,900 | 17,300 | 17,800 | 18,100 | 18,100 |
| Mean EV battery capacity [kWh] | 60 | 70 | 80 | 90 | 100 |
| Total household electricity demand [TWh] (inc. heat pump, exc. PVs and EVs) | 82 | 88 | 99 | 91 | 83 |

The implemented control strategies use the EV charging pole arrival and departure times in different ways. The EV arrival times are not considered in the rule-based controller as the

controller does not need this information to employ basic implementation of the charging strategies. However, the EV charging pole departure times are taken into account without uncertainty in the rule-based control algorithm to reduce the user range anxiety through ensuring full EV batteries upon departure as explained in Section 3-2-3. As the (scenario-based) MPC algorithm has the ability to take into account simulated future values, it is assumed that the EV charging pole arrival times are also known without uncertainty by the algorithm. In addition to the arrival times, the MPC algorithm also knows the EV battery state of charge (SOC) at the future arrival time. These assumptions are made to not further increase the microgrid model complexity. Similar to the rule-based controller, the MPC algorithm takes into account the EV departure times to ensure full EV batteries at charging pole departure.

A prediction horizon N_h of one day is chosen for the MPC algorithms such that the daily cyclic behavior of variables is taken into account, e.g. EV charging pole departures at the next day and no PV generation during the night opposed to generation during the day. The prediction horizon is not chosen as a longer period to keep the computation time of the optimal control problem low. The sampling time is set to 15 minutes as this is largest time between measurements of the available data, i.e. the electricity price, the household loads, and the PV generation.

The simulations are executed using Matlab R2017a software together with the Gurobi 8.1 solver to address the mixed integer linear programming (MILP) problem. A MacBook Pro 2015 computer with 2.5 GHz Intel Core i7 processor, 16 GB 1600 MHz DDR3 memory, and AMD Radeon R9 M370X 2048 MB Intel Iris Pro 1536 MB graphics card is used for simulations. To give an indication of the computation time: a two week simulation of a V2H charging strategy for 106 EVs using MPC takes approximately 14.5 hours.

4-2 Case study 1: comparing electric vehicle charging strategies

This aim of this case study is to investigate which charging strategy, i.e. uncontrolled charging, smart charging, or V2H charging is the most effective in reducing the economical household costs. This is achieved through simulating the charging strategies using a rule-based controller and a MPC algorithm. The MPC algorithm is implemented in a perfect information case and certainty equivalent case. A microgrid simulation period of two weeks is chosen to take into account the weekend period while keeping the computation time of the simulations low. The results of the simulations are compared and conclusions are drawn at the end of this section.

The effects of seasonal dependent variables, i.e. PV generation and household loads, on the economical costs reduction are taken into account in this case study through the simulation of extreme seasonal cases, see Section 2-3 and Section 2-4. The case where there is maximal PV generation together with minimum household demand is denoted as the summer season. On the other hand, the winter season represents minimum PV generation together with maximum household loads. Finally, the median season depicts the median (i.e. middle value of an ordered set) PV generation together with a median household load, which could represent a case during either spring or autumn. Note that these simulations depict extreme cases e.g. the PV generation is not necessary high each day in the summer. The electricity price does not have seasonal effects, therefore, the period of the extracted PV generation data is also chosen as period for the electricity prices in each season.

It is observed that the PV generation in the New Orleans 2040 microgrid case never exceeds the household load. However, in other microgrid cases it could occur that more PV power is generated than the current household demand. Therefore, an extra summer simulation is included where the PV power is three times higher than normal, this case is denoted as the 3 · PV summer simulation. The PV generation is roughly 1.5 times the household load during maximum production in the 3 · PV summer simulation.

4-2-1 Results

Table 4-2 shows the simulation results of the summer season of the microgrid case study. The headers indicate the implemented charging strategy, i.e. uncontrolled charging, smart charging, or V2H charging, using a specific control algorithm, i.e. rule-based or MPC using perfect information (PI) or certainty equivalent (CE). The first column depicts the total and the specific microgrid cost elements. As explained in Section 3-5-2, the total microgrid costs consists of a weighted summation of the economical costs (i.e. electricity costs and the distributed system operator (DSO) costs due to the peak power demand to the grid), and the full EV battery shortage at charging pole departure costs. The total costs are compared first to analyze the performance of the control strategies. The costs elements are compared thereafter to investigate the effectiveness of the charging strategies in view of the improvements for the households.

Table 4-2: Comparing EV charging strategies simulation results of summer season.

| | Uncontrolled | | Smart | | V2H | | |
|----------------------------------|--------------|--------|--------|--------|------------|--------|--------|
| | Rule-based | | MPC | | Rule-based | MPC | |
| | | | CE | PI | | CE | PI |
| Total costs | 14019 | 14565 | 2958 | 2925 | 15744 | 2968 | 2904 |
| Economical costs [€] | 3429 | 3223 | 3256 | 3197 | 3326 | 3283 | 3210 |
| Electricity costs [€] | 2619 | 2498 | 2512 | 2480 | 2514 | 2518 | 2454 |
| due to EVs | 681 | 559 | 573 | 542 | 944 | 684 | 655 |
| Peak power [kW] | 319 | 241 | 258 | 232 | 306 | 273 | 265 |
| Mean EV departure shortage [kWh] | 0 | 8.4384 | 0.0040 | 0.0041 | 9.2675 | 0.0032 | 0.0034 |

Total costs comparison

It is observed that implementation of smart charging or V2H charging using rule-based control results in higher total costs compared to uncontrolled charging. This is due to the fact that the rule-based control implementation for smart charging and V2H charging is less effective in filling up the EV to 100 % SOC for charging pole departure compared to uncontrolled charging.

The mean EV departure shortage is always zero using uncontrolled charging. This is because the EV charging pole arrival and departure times are assigned such that an EV always has enough time to charge its daily energy demand.

As expected, when considering the total costs of either smart charging or V2H charging, the MPC algorithm always shows a better performance than the rule-based control algorithm through which the perfect information model always has the best performance. In addition, the V2H implementation using perfect information MPC has the lowest total microgrid costs compared to all other implemented control and charging strategies.

Furthermore, V2H charging using either rule-based control or certainty equivalent MPC is less effective in reducing the total costs than the smart charging counterpart control algorithms. This is due to the fact that V2H charging enables a bidirectional power flow through the power converter in the EV. The power flow conversion, i.e. AC-to-DC or vice versa, is associated with energy losses as explained in Section 2-2-2. The potential cost savings of discharging the EVs to support the household loads due to, e.g. current expensive electricity prices, should outweigh the costs of importing extra electricity to compensate extra conversion losses at a later time instant. This dilemma can only be taken into account effectively through the control algorithm if the forecasts of uncertain variables, i.e. the PV generation, the household loads, and the electricity prices, are of high quality. The V2H rule-based control implementation will therefore always perform worse than the smart charging counterpart as the algorithm does not take forecasts of uncertain variables into account. Although the MPC algorithm does take expected developments of uncertain variables into account, the results show that the certainty equivalent case still fails to outperform the smart charging counterpart in decreasing the total costs. Table 4-3 presents the simulation results of the summer season with the assumption that the EV power conversion is 100 % efficient, i.e. no energy is lost during charging or discharging. The results show that in this case, the certainty equivalent MPC V2H charging manages to outperform both the rule-based and certainty equivalent MPC smart charging implementations.

Table 4-3: Comparing EV charging strategies simulation results of summer season assuming no EV power conversion losses.

| | Uncontrolled | | Smart | | V2H | | |
|-------------------------------------|--------------|--------|--------|--------|------------|--------|--------|
| | Rule-based | | MPC | | Rule-based | MPC | |
| | | | CE | PI | | CE | PI |
| Total costs | 13939 | 14348 | 2886 | 2853 | 15299 | 2796 | 2659 |
| Economical costs [€] | 3342 | 3157 | 3180 | 3119 | 3148 | 3251 | 3138 |
| Electricity costs [€] | 2553 | 2445 | 2451 | 2420 | 2373 | 2350 | 2211 |
| due to EVs | 614 | 507 | 513 | 482 | 826 | 995 | 1035 |
| Peak power [kW] | 309 | 238 | 253 | 226 | 296 | 410 | 437 |
| Mean EV departure shortage [kWh] | 0 | 8.3270 | 0.0032 | 0.0032 | 9.0659 | 0.0028 | 0.0028 |

Table 4-4 shows the results of the median season, winter season, and 3 · PV summer season simulations. The results show no new important information compared to the aforementioned observations of the summer season simulation. The differences in costs are due to the differences of household energy demand, PV generation, and electricity prices throughout the year.

Table 4-4: Comparing EV charging strategies simulation results of the 3 · PV case, median season, and winter season.

| | Uncontrolled | Smart | | | V2H | | |
|----------------------------------|--------------|------------|--------|--------|------------|--------|--------|
| | | Rule-based | MPC | | Rule-based | MPC | |
| | | | CE | PI | | CE | PI |
| 3 · PV summer | | | | | | | |
| Total costs | 12958 | 13445 | 1915 | 1875 | 14343 | 1916 | 1841 |
| Economical costs [€] | 2364 | 2189 | 2204 | 2132 | 2223 | 2223 | 2100 |
| Electricity costs [€] | 1710 | 1602 | 1621 | 1583 | 1596 | 1616 | 1545 |
| due to EVs | 562 | 457 | 471 | 422 | 638 | 533 | 475 |
| Peak power [kW] | 296 | 233 | 232 | 203 | 268 | 255 | 214 |
| Mean EV departure shortage [kWh] | 0 | 8.3848 | 0.0037 | 0.0040 | 9.0334 | 0.0033 | 0.0033 |
| Median | | | | | | | |
| Total costs | 15001 | 15506 | 3923 | 3894 | 16893 | 3945 | 3870 |
| Economical costs [€] | 4458 | 4199 | 4274 | 4179 | 4320 | 4347 | 4203 |
| Electricity costs [€] | 3542 | 3412 | 3416 | 3393 | 3429 | 3431 | 3361 |
| due to EVs | 802 | 671 | 676 | 653 | 1218 | 798 | 812 |
| Peak power [kW] | 365 | 246 | 311 | 245 | 325 | 361 | 291 |
| Mean EV departure shortage [kWh] | 0 | 8.4168 | 0.0042 | 0.0039 | 9.3930 | 0.0034 | 0.0035 |
| Winter | | | | | | | |
| Total costs | 14301 | 15161 | 3373 | 3364 | 16709 | 3380 | 3310 |
| Economical costs [€] | 3921 | 3703 | 3728 | 3632 | 3815 | 4096 | 3669 |
| Electricity costs [€] | 2888 | 2782 | 2765 | 2762 | 2772 | 2731 | 2692 |
| due to EVs | 521 | 416 | 398 | 396 | 864 | 690 | 593 |
| Peak power [kW] | 385 | 281 | 320 | 234 | 372 | 678 | 323 |
| Mean EV departure shortage [kWh] | 0 | 8.5513 | 0.0076 | 0.0078 | 9.6604 | 0.0074 | 0.0072 |

Cost elements comparison

Figure 4-2 shows the economical cost decrease compared to uncontrolled charging in the summer season. The results show that the rule-based control implementation of smart charging has a larger economical cost decrease compared to the certainty equivalent MPC implementation of smart charging. On the other hand, rule-based V2H charging performs worse than the certainty equivalent MPC implementation of V2H. However, the outperformance of rule-based control over certainty equivalent MPC, or vice versa, in view of one charging strategy is not fixed as different seasons show contrasting results. These different results are attributed to the objective function of the MPC. First of all, the economical cost decrease of the MPC algorithm could be improved through tuning the weights in the objective function such that more priority is given to reduce the economical costs than to maximize the SOC of the EV

at charging pole departure. Tuning the weights differently could therefore result into e.g. certainty equivalent MPC outperforming the economical cost reduction of rule-based control in view of smart charging. Furthermore, the mean values of uncertain variables in the MPC objective function, e.g. the electricity price and the household loads, vary throughout the year which affects the ratio between the different costs in the objective function. As a result, different optimizations priorities are given to the costs in the objective function without changing the weights. In conclusion, it cannot be deduced from the results if either a rule-based control or a certainty equivalent MPC implementation gives the best economical cost decrease in view of one charging strategy.

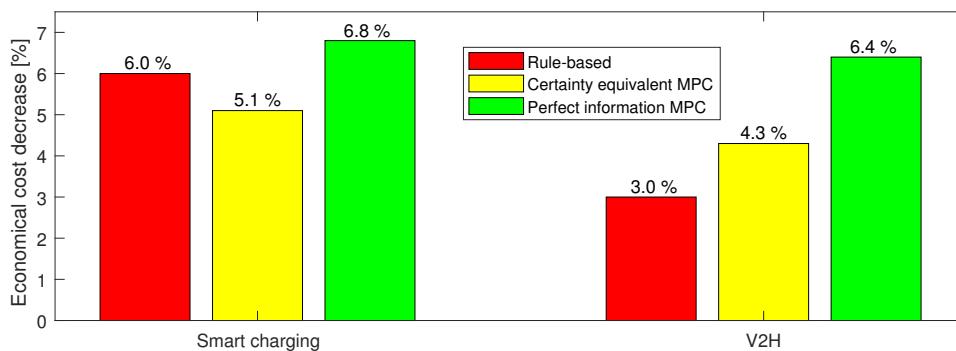


Figure 4-2: Economical microgrid costs decrease compared to uncontrolled charging in summer.

However, it is not expected that weight changes in the MPC objective function will result in higher economical cost reductions for certainty equivalent MPC V2H compared to the certainty equivalent MPC smart charging implementation since the total microgrid costs of the certainty equivalent MPC V2H implementation are always higher than the smart charging counterpart. Furthermore, the rule-based controller of V2H has always higher economical costs than the smart charging implementation.

The results show further that a rule-based smart charging implementation already gives a substantial economical cost reduction compared to the other implementations.

4-2-2 Conclusions

Although V2H can outperform smart charging in some cases, e.g. when comparing total cost using perfect information MPC, it often fails to do so as the persistence forecast model prediction is not accurate enough to compensate the costs of increased EV power efficiency losses. In addition, a simple smart charging rule-based control algorithm can already reduce the economical costs with respect to using uncontrolled charging significantly. Moreover, the implementation of V2H is more involved than smart charging as explained in Section 2-2-2. It is therefore concluded that smart charging is the most effective charging strategy to reduce the economical microgrid costs in practice.

4-3 Case study 2: comparing scenario generation strategies

The aim of this case study is to investigate if the total microgrids costs, considering smart charging, can be reduced more than the certainty equivalent MPC algorithm by taking into account the uncertainty of the electricity prices, the household loads, and the PV generation. The potential uncertainty is taken into account through implementing and comparing six scenario generation methods:

- Yearly error variable
- Yearly error constant
- Daily error variable
- Daily error constant
- Seasonal hourly error
- Matching profile

in a scenario-based MPC algorithm. Smart charging is considered as the previous case study concluded that it is the most effective charging strategy for reducing the economical microgrid costs in practice.

The previous case study is adapted to fit the needs of this case study. A simulation is done for one week and for 25 EVs to prevent high computation times for the simulation. The uncontrolled charging and smart charging strategies are simulated using rule-based control and MPC using a perfect information and certainty equivalent case as performance benchmarks.

All data of the uncertain variables which is not used for simulation is used to initialize the historical forecast error histograms of the scenario generation methods, see Section 3-6-1. The median season is therefore chosen as simulation period in this case study to ensure that the error histogram contains data of different seasons. Only one year worth of data is available for simulating the uncertain variables. Consequently, the scenarios are generated also using forecast errors which would only be available in the period after the simulation, e.g. simulation is in march but error distribution of scenario generation method contains data from April in the same year. However, it is not expected that this data approach has a significant effect on the results as the uncertain variables show generally similar behavior in seasons when comparing different years, e.g. roughly similar household loads in the summer of the year 2018 compared to the summer of the year 2019.

The simulations are done while using one scenario generation method for all uncertain variables simultaneously. It is possible that one scenario generation method works better for a specific uncertain variable e.g. the household loads, but worse for another. Investigating which scenario generation method works best for which uncertain variable is therefore suggested as topic for further research.

The relation between the performance of the scenario-based MPC and the number of generated scenarios is also taken into account through simulating for an increasing number of generated scenarios, i.e. 5, 10, 20, 40, 80, and 160 scenarios.

4-3-1 Results

Figure 4-3 shows the total microgrid costs after simulating the smart charging strategy using six scenario generation methods for a varying number of scenarios in the scenario-based MPC algorithm. The dashed lines in the figure shows the benchmark performance of rule-based control and MPC implementations. Note that the y-axis of the figure does not start at zero to improve the visibility of the different results. The same results are also shown in Figure 4-4 only up to a lower number of scenarios such that the performance differences of the different methods are better distinguishable.

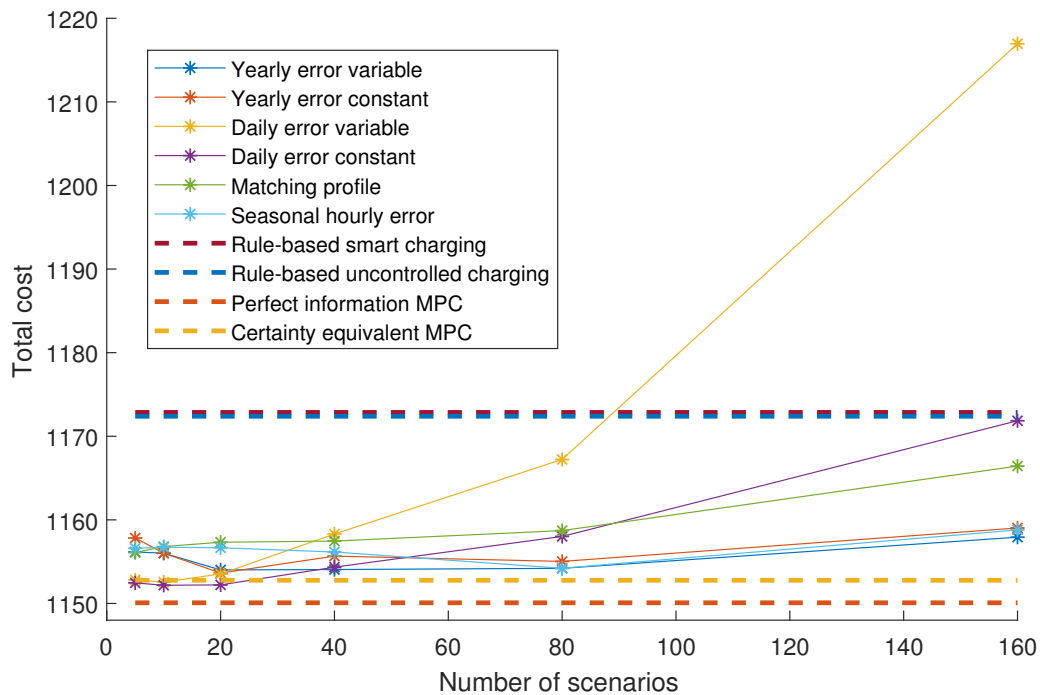


Figure 4-3: Total cost comparison of scenario generation methods using scenario-based MPC.

Figure 4-3 shows that the total cost increases for all scenario generation methods as the number of scenarios grows. This trend is explained through the quality difference between the persistence forecast model and the generated scenarios. The implemented scenarios in the scenario-based MPC consist of the persistence forecast, i.e. the best available prediction of the uncertain variables, and additional generated scenarios using a scenario generation method. Each scenario generation method has a different assumption on the uncertainty, however, these assumptions are all considered to be simplistic, e.g. a stationary assumption on the error distribution while the household load shows seasonal differences. The performance of the scenario-based MPC is therefore worsened when the emphasis is put too much on finding an optimal control action based on the generated scenarios than on the persistence forecast, i.e. implementing a high number of scenarios.

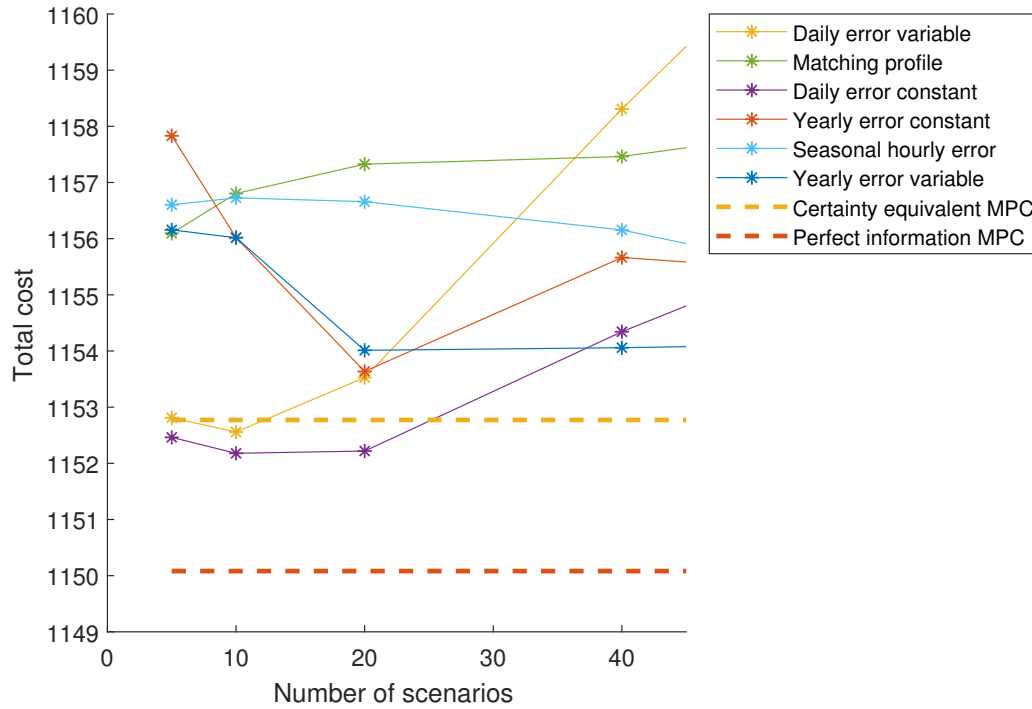


Figure 4-4: Zoomed in: total cost comparison of scenario generation methods using scenario-based MPC.

Furthermore, the results show that each scenario generation method has an optimum number of scenarios for which the scenario-based MPC gives the best performance. For instance, the daily error variable generation method performs best using ten scenarios while the seasonal hourly error generation method has its optimum when using eighty scenarios. This difference is attributed to the characteristics of the scenario generation methods of which most methods use collected forecast errors based on either long periods of data, i.e. yearly or seasonal, or on short periods of data, i.e. daily. The short-term error data encapsulates more the temporary uncertainty effects, i.e. the collected persistence forecast error distribution is prone to change often. The emphasis on the short-term error data compared to the single persistence forecast should therefore be kept low in the scenario-based MPC algorithm to prevent relying too much on a dynamic error distribution data. This is visible in Figure 4-3 as the performance of short-term based scenario generation methods deteriorates quickly, faster than the long-term error based generation methods, when the number of scenarios is increased. On the other hand, the total costs of the long-term scenario generation methods rise much more slower than the short-term methods when increasing the number of implemented scenarios. Following the similar reasoning as the short-term performance, the long-term scenario generation methods encapsulates longer temporal uncertainty effects, i.e. the collected persistence forecast changes slowly. Therefore, reasonable optimization performance is still achieved when more emphasis is given on the generated scenarios instead of the persistence forecast.

Although the minimum number of generated scenarios is five, the matching profile scenario generation method seems to have the best performance when generating as few scenarios as possible. This is an indication that similar looking historical profiles of uncertain variables

do not have a high probability of having similar future profiles.

No generalizations can be made on differences between scenario generation methods which add the error drawn from the error distribution as a constant or as a variable to the persistence forecast.

Almost all scenario generation methods fail to outperform the certainty equivalent MPC total microgrid costs except for both the daily error constant and daily error variable scenario generation methods while using a small number of generated scenarios. The results show that the best performance is achieved by generating ten scenarios with the use of the daily error constant scenario generation method. It is possible that the true optimal needed number of generated scenarios is slightly higher or lower than ten for the daily error constant method. More simulations have to be done to find this optimum more precisely.

4-3-2 Conclusions

All scenario generation methods have higher total microgrid costs when the number of implemented scenarios increases. Furthermore, each scenario generation method has an optimal number of scenarios for which that method gives the best performance. A higher optimum number is related to scenario generation methods which are based on long-term forecast error collection, e.g. yearly or seasonal, a lower optimum number is related to short-term forecast error collection methods. Finally, all scenario generation methods, except for the daily error methods, fail to outperform the total microgrid costs of the certainty equivalent MPC. The best performance is achieved through using the daily error constant scenario generation and generating a low number of scenarios.

4-4 Conclusions

This chapter presented a description of two case studies after which the results and conclusions were discussed. The aim of the first case study was to find out which charging strategy, i.e. uncontrolled charging, smart charging, or V2H charging is the most effective in reducing the economical microgrid costs. The charging strategies were implemented through a rule-based control and a MPC algorithm considering a certainty equivalent and a perfect information case. It was concluded that the smart charging strategy is the most effective charging strategy in practice. Although V2H charging strategy is able to reduce the economical costs more in some cases, i.e. using perfect information MPC, the performance is highly dependent on the quality of the forecast of the uncertain variables which often is insufficient. The aim of the second case study was to investigate if the total microgrid costs of certainty equivalent MPC, considering smart charging, could be reduced further through a scenario-based MPC algorithm. Six scenario generations methods were compared and simulated while varying the number of generated scenarios. It was concluded that the total microgrid costs of smart charging can be reduced further through implementing a daily error scenario generation method and generating a low number of scenarios for the scenario-based MPC.

Conclusions and recommendations

5-1 Summary and conclusions

The expected increase of electric vehicle (EV) adoption poses potential problems for the distributed system operator (DSO), who is responsible for maintaining the grid. It is expected that the increase in electricity demand, partially induced through EVs, will cause peak loads that will possibly result in grid deterioration or outages. A promising solution is to employ different charging strategies for EVs. Therefore, the aim of this research is to compare uncontrolled charging, smart charging, and vehicle-to-home (V2H) charging in a microgrid on their economical effect for their users. The economical microgrid costs consist of the electricity costs and the DSO costs which depend on the peak load to the main grid. The charging strategies are implemented using a simple rule-based controller and a model predictive control (MPC) algorithm which is able to take future values of variables into account, e.g. photovoltaic (PV) generation. The MPC algorithm is implemented using a perfect information case, i.e. the PV generation of tomorrow is forecasted perfectly, and a certainty equivalent case using a persistence forecast model, i.e. it is assumed that the PV generation of tomorrow is equal to that of today.

The results show that V2H charging can decrease the economical microgrid costs more than smart charging in theory. However, it is difficult to achieve this performance as it is strongly dependent on the quality of the forecasts of the uncertain variables, i.e. the electricity price, the household loads, and the PV generation. The quality of the forecasts needs to be high as V2H charging will risk increased power conversion losses through discharging the EV with the aim to lower the economical microgrid costs. Furthermore, the implementation costs are higher for V2H charging than for smart charging as most commercial EVs and charging poles only support unidirectional charging. It is therefore concluded that smart charging is the most effective charging strategy. Furthermore, a simple rule-based control implementation of smart charging can already reduce the economical microgrid costs significantly.

Additional research is done to investigate if the total microgrid costs can be reduced further through taking into account uncertain variables. A scenario-based MPC algorithm is used

for its ability to consider multiple forecasts of an uncertain variable. Since there is only one forecast available from the persistence forecast model, six different scenario generation methods are used to compare on performance. Most scenario generation methods generate scenarios using the historical forecast error of different periods, i.e. yearly, daily, or hourly, and through adding the error either as a constant or as a variable to the persistence forecast model. Microgrid simulations are done while varying the number of implemented scenarios in the scenario-based MPC.

The results show that each scenario generation method has an optimal number of scenarios for which that method gives the best performance. However, the total costs of all scenario generation methods keeps increasing when more scenarios are implemented than the optimum number. A higher optimum number of implemented scenarios is related to scenario generation methods which are based on long-term forecast error collection, e.g. of the past year or season, a lower optimum number is related to short-term forecast error collection methods, e.g. of the past day. Finally, all scenario generation methods, except for the daily error methods, fail to outperform the total microgrid costs of the certainty equivalent MPC. The best performance is achieved through using the daily error fixed scenario generation and generating a low number of scenarios.

5-2 Discussion and future work

Several discussion points and suggestions for further work arose during this thesis and are presented in this section.

The electricity price is, among others factors, based on the demand and supply of electricity as discussed in Section 2-1-3. The electricity price would therefore be effected if other microgrids would also implement smart charging or V2H charging. The extra demand for cheaper electricity prices will increase the electricity rates which will reduce the potential economical cost decrease for microgrids. It seems therefore that early adopters of smart charging or V2H charging will have a larger financial benefit than users who will implement smart charging at a later stage.

The simulations in this research are based on a residential microgrid where most EVs are not available during the day as they are being used for transportation for going to e.g. work. Therefore, there is not much opportunity in the microgrid to store possible excess generated PV energy during the day in EVs. As a result, the excess energy is sold back to the grid for a relative low price. Therefore, it is interesting to consider a microgrid in a business context in which EVs are available throughout the day not during the night, e.g. a shopping mall or a business park.

It is shown in this research that the economical microgrid costs due to uncontrolled charging can be reduced with 6.8 % in the summer using smart charging in a perfect information MPC case, see Figure 4-2. This would amount to a saving per EV of € 2.19 in two weeks. However, the economical cost reduction could be higher in reality as taxes and the electricity supplier overhead costs are not taken into account in this research as explained in Section 2-1-3. Furthermore, through changing the weights in the MPC cost function, more preference could be given to economical cost reduction than to ensuring that the EV has a full battery at departure. This weighting is up to the user as it is a trade-off between financial benefits

and comfort. A suggestion for future work is to investigate if the potential financial benefits due to smart charging are worth the investments costs of implementing the smart charging strategy.

The scenario generation methods are applied on all uncertain variables, e.g. the electricity price, the household loads, and the PV generation, simultaneously during simulating the second case study. However it is possible that one scenario generation method could perform better for a specific uncertain variable and worse for another. It is therefore suggested for further research to investigate how the scenario generation methods affect the scenario-based MPC performance when different methods are used for different uncertain variables.

5-3 Advice to distributed system operator

The DSO faces the major challenge of maintaining the electricity grid during the energy transition. Some potential grid problems such as the increasing peak power demand are partially attributed to the increased use of EVs that are charged using an uncontrolled charging strategy. This research compares uncontrolled charging, smart charging, and V2H charging on their economical effects, i.e. the electricity price and the DSO costs attributed to the peak power demand, for their users in a microgrid. The results show that smart charging is the most effective charging strategy in practice as V2H charging brings higher implementation costs and its potential extra economical cost decrease is highly dependent on the forecast quality of uncertain variables, e.g. the electricity price. Furthermore, a significant economical cost reduction is already achieved through the implementation of a simple rule-based controller, therefore, it is probably not worth the extra investment costs to implement smart charging using a sophisticated control algorithm such as MPC. The question remains however if the potential economical savings for the microgrid households are sufficient considering the smart charging implementation investment costs. Nevertheless, the DSO should encourage the implementation of residential smart charging strategies as it will result in lower peak demands to the grid compared to uncontrolled charging.

Appendix A

Reformulation of electric vehicle battery dynamics

Full elaboration of the reformulation of the piecewise linear battery dynamics using the mixed logical dynamical (MLD) framework, see Section 3-2-1 and 3-3 [3].

The battery dynamics are defined as a piecewise linear model:

$$x(k+1) = \begin{cases} \text{A} := x(k) - E^{\text{dem}} & \text{if } \delta^c(k) = 1 \wedge \delta^c(k+1) = 0 \\ \text{B} := x(k) + T_s \eta P^{\text{EV}}(k) & \text{if } \delta^c(k) = 1 \wedge \delta^c(k+1) = 1 \\ \text{C} := x(k) & \text{if } (\delta^c(k) = 0 \wedge \delta^c(k+1) = 0) \dots \\ & \vee (\delta^c(k) = 0 \wedge \delta^c(k+1) = 1). \end{cases}$$

The following auxiliary variables and constraints are introduced:

$$\delta^{\text{EV}}(k) = 1 \iff P^{\text{EV}}(k) \geq 0 \quad \text{is true iff } \begin{cases} -\underline{P}^{\text{EV}} \delta^{\text{EV}}(k) \leq P^{\text{EV}}(k) - \underline{P}^{\text{EV}} \\ -(\bar{f} + \epsilon) \delta(k) \leq -f(k) - \epsilon \end{cases}$$

$$z^{\text{EV}}(k) = \delta^{\text{EV}}(k) P^{\text{EV}}(k) \quad \text{is equivalent to } \begin{cases} z^{\text{EV}}(k) \leq \bar{P}^{\text{EV}} \delta^{\text{EV}}(k) \\ -z^{\text{EV}}(k) \leq -\underline{P}^{\text{EV}} \delta^{\text{EV}}(k) \\ z^{\text{EV}}(k) \leq P^{\text{EV}}(k) - \underline{P}^{\text{EV}}(1 - \delta^{\text{EV}}(k)) \\ -z^{\text{EV}}(k) \leq -P^{\text{EV}}(k) + \bar{P}^{\text{EV}}(1 - \delta^{\text{EV}}(k)), \end{cases}$$

and used to rewrite the B part of the battery dynamics:

$$\begin{aligned}
B &:= \delta^{P^{EV}}(k) \left(x(k) + T_s \eta^c P^{EV}(k) - x^{pl} \right) + \left(1 - \delta^{P^{EV}}(k) \right) \left(x(k) + \frac{T_s}{\eta^d} P^{EV}(k) \right) \\
&:= \delta^{P^{EV}}(k) T_s \eta^c P^{EV}(k) + x(k) + \frac{T_s}{\eta^d} P^{EV}(k) - \frac{T_s}{\eta^d} P^{EV}(k) \delta^{P^{EV}}(k) \\
&:= z^{EV}(k) T_s \eta^c + x(k) + \frac{T_s}{\eta^d} P^{EV}(k) - \frac{T_s}{\eta^d} z^{EV}(k) \\
&:= T_s \left(\eta^c - \frac{1}{\eta^d} \right) z^{EV}(k) + \frac{T_s}{\eta^d} P^{EV}(k) + x(k).
\end{aligned} \tag{A-1}$$

The battery dynamics are now rewritten into a single mixed integer linear programming (MILP) equation using the electric vehicle (EV) connected indicators considering the model parts:

$$\begin{aligned}
x(k+1) &= \delta^c(k) \left(\delta^c(k+1) B + (1 - \delta^c(k+1)) A \right) + (1 - \delta^c(k)) C \\
&= \delta^c(k) \delta^c(k+1) (B - A) + \delta^c(k) (A - C) + C \\
&= \delta^c(k) \delta^c(k+1) \left(T_s \left(\eta^c - \frac{1}{\eta^d} \right) z^{EV}(k) + \frac{T_s}{\eta^d} P^{EV}(k) + x(k) - x(k) + E^{\text{dem}} \right) + \\
&\delta^c(k) \left(x(k) - E^{\text{dem}} - x(k) \right) + x(k) \\
&= \delta^c(k) \delta^c(k+1) \left(T_s \left(\eta^c - \frac{1}{\eta^d} \right) z^{EV}(k) + \frac{T_s}{\eta^d} P^{EV}(k) + E^{\text{dem}} \right) - \\
&\delta^c(k) E^{\text{dem}} + x(k).
\end{aligned} \tag{A-2}$$

Bibliography

- [1] Beek, K., Bontenbal, H., Melle, T. v., and Terlouw, W. (2017). Scenariostudie stedin ecofys: samenleving & energiemarkt in 2050. Report.
- [2] Belastingdienst, (2019). Tabellen tarieven milieubelastingen. https://www.belastingdienst.nl/wps/wcm/connect/bldcontentnl/belastingdienst/zakelijk/overige_belastingen/belastingen_op_milieugrondslag/tarieven_milieubelastingen/tabellen_tarieven_milieubelastingen.
- [3] Bemporad, A. and Morari, M. (1999). Control of systems integrating logic, dynamics, and constraints. *Automatica*, 35(3):407–427.
- [4] Bidram, A. and Davoudi, A. (2012). Hierarchical structure of microgrids control system. *IEEE Transactions on Smart Grid*, 3(4):1963–1976.
- [5] Brinkel, N., Borning, M., Ketov, M., Klingsch, G., and Mann, P. (2017). Tennet market review 2017. Report.
- [6] Camacho, E. and Bordons, C. (2007). *Model Predictive Control*, volume 13 of *Advanced Textbooks in Control and Signal Processing*. Springer-Verlag London, 2nd edition.
- [7] Centraal Bureau voor de Statistiek, (2017a). Mean yearly driven distances with cars in the Netherlands. <https://statline.cbs.nl/Statweb/publication/?DM=SLNL&PA=83703NED&D1=a&D2=0&D3=0,4-5&D4=1&HDR=T&STB=G3,G2,G1&VW=T>.
- [8] Centraal Bureau voor de Statistiek, (2017b). Percentiles of yearly driven distances with cars in the Netherlands. www.cbs.nl.
- [9] Cuijpers, M., Staats, M., Bakker, W., and Hoekstra, A. (2016). Ecofys: Toekomstverkenning elektrisch vervoer. Report.
- [10] ENTSO-E Transparency Platform, (2018). Day-ahead prices. <https://transparency.entsoe.eu/transmission-domain/r2/dayAheadPrices/show>.
- [11] Geske, J. and Schumann, D. (2018). Willing to participate in vehicle-to-grid (V2G)? why not! *Energy Policy*, 120:392–401.

- [12] Google Earth, (2019). New orleans building in rotterdam. <https://earth.google.com>.
- [13] Hato, Y., Chien, H. C., Hirota, T., Kamiya, Y., Daisho, Y., and Inami, S. (2015). Degradation predictions of lithium iron phosphate battery. *World Electric Vehicle Journal*, 7:25–31.
- [14] Hatziargyriou, N., Asano, H., Iravani, R., and Marnay, C. (2007). Microgrids. *IEEE Power and Energy Magazine*, 5(4):78–94.
- [15] Heirung, T. A. N., Paulson, J. A., O’Leary, J., and Mesbah, A. (2018). Stochastic model predictive control — how does it work? *Computers Chemical Engineering*, 114:158–170.
- [16] Kempton, W. and Tomić, J. (2005). Vehicle-to-grid power fundamentals: Calculating capacity and net revenue. *Journal of Power Sources*, 144(1):268–279.
- [17] Langen, S. v., Tol, P. v., Quak, T., Sinke, M., and Bruggen, M. v. (2018). Profielen elektriciteit 2018. <https://www.nedu.nl/documenten/verbruiksprofielen/>.
- [18] Liu, C., Chau, K. T., Wu, D., and Gao, S. (2013). Opportunities and challenges of vehicle-to-home, vehicle-to-vehicle, and vehicle-to-grid technologies. *Proceedings of the IEEE*, 101(11):2409–2427.
- [19] Mies, J., Helmus, J., and van den Hoed, R. (2018). Estimating the charging profile of individual charge sessions of electric vehicles in the netherlands. *World Electric Vehicle Journal*, 9(2):17.
- [20] Mohammadi, S., Soleymani, S., and Mozafari, B. (2014). Scenario-based stochastic operation management of microgrid including wind, photovoltaic, micro-turbine, fuel cell and energy storage devices. *International Journal of Electrical Power Energy Systems*, 54:525–535.
- [21] Mwasilu, F., Justo, J. J., Kim, E.-K., Do, T. D., and Jung, J.-W. (2014). Electric vehicles and smart grid interaction: A review on vehicle to grid and renewable energy sources integration. *Renewable and Sustainable Energy Reviews*, 34:501–516.
- [22] Nibud (2018). Average household yearly electricity use in the netherlands.
- [23] Olivares, D. E., Cañizares, C. A., and Kazerani, M. (2014a). A centralized energy management system for isolated microgrids. *IEEE Transactions on Smart Grid*, 5(4):1864–1875.
- [24] Olivares, D. E., Mehrizi-Sani, A., Etemadi, A. H., Cañizares, C. A., Iravani, R., Kazerani, M., Hajimiragha, A. H., Gomis-Bellmunt, O., Saeedifard, M., Palma-Behnke, R., Jiménez-Estévez, G. A., and Hatziargyriou, N. D. (2014b). Trends in microgrid control. *IEEE Transactions on Smart Grid*, 5(4):1905–1919.
- [25] Parisio, A., Rikos, E., and Glielmo, L. (2014a). A model predictive control approach to microgrid operation optimization. *IEEE Transactions on Control Systems Technology*, 22(5):1813–1827.
- [26] Parisio, A., Varagnolo, D., Molinari, M., Pattarello, G., Fabietti, L., and Johansson, K. H. (2014b). Implementation of a scenario-based mpc for hvac systems: an experimental case study. *IFAC Proceedings Volumes*, 47(3):599–605.

- [27] Pellis, J. (2018). Position paper stedin: Samen sterk werk maken van een flexibel energie systeem.
- [28] Refa, N. (2019). Twenty thousand full electric vehicle charging sessions from public charging poles in the netherlands. www.elaad.nl.
- [29] Sadeghianpourhamami, N., Refa, N., Strobbe, M., and Develder, C. (2018). Quantitive analysis of electric vehicle flexibility: a data-driven approach. *Electrical Power & Energy Systems*, 95:451–462.
- [30] Schildbach, G., Fagiano, L., Frei, C., and Morari, M. (2014). The scenario approach for stochastic model predictive control with bounds on closed-loop constraint violations. *Automatica*, 50(12):3009–3018.
- [31] Sen, S. and Kumar, V. (2018). Microgrid control: A comprehensive survey. *Annual Reviews in Control*, In review available online.
- [32] Stedin (2018). Electriciteit tarieven 2018: Aansluiting en transport voor kleinverbruikers.
- [33] Stedin (2019). Elecktriciteitstarieven 2019: Aansluiting en transport voor grootverbruikers.
- [34] Stocker, T. (2014). *Climate change 2013: the physical science basis: Working Group I contribution to the Fifth assessment report of the Intergovernmental Panel on Climate Change*. Cambridge University Press.
- [35] TE Bulletin: News from the European Federation for Transport and Environment, (2006). Who adds pressure for stricter euro-5 standards.
- [36] Tractabel (Engie), (2018). Elaad: Optimale integratie van elektrisch vervoer, pv, warmtepompen in bestaand energiesysteem - executive summary. Report.
- [37] Yong, J. Y., Ramachandaramurthy, V. K., Tan, K. M., and Mithulananthan, N. (2015). A review on the state-of-the-art technologies of electric vehicle, its impacts and prospects. *Renewable and Sustainable Energy Reviews*, 49:365–385.

Glossary

List of acronyms

| | |
|-----------------------|----------------------------------|
| AC | alternating current |
| CE | certainty equivalent |
| DC | direct current |
| DSO | distributed system operator |
| EMS | energy management system |
| ESS | energy storage system |
| EV | electric vehicle |
| Li-ion | lithium-ion |
| MILP | mixed integer linear programming |
| MLD | mixed logical dynamical |
| MPC | model predictive control |
| PCC | point of common coupling |
| PI | perfect information |
| PV | photovoltaic |
| SOC | state of charge |
| VA_r | volt-ampere reactive |
| V2G | vehicle-to-grid |
| V2H | vehicle-to-home |
| V2V | vehicle-to-vehicle |
| V2X | vehicle-to-everything |

List of symbols

| | |
|---------------------|---|
| $\bar{\cdot}$ | Maximum value |
| δ^c | EV connected indicator |
| δ^{PEV} | Positive EV power indicator |
| η | EV power conversion efficiency |
| η^c | EV charge efficiency |
| η^d | EV discharge efficiency |
| $\underline{\cdot}$ | Minimum value |
| c^p | Purchase price of grid electricity [€] |
| c^s | Selling price of grid electricity [€] |
| C^{DSO} | DSO costs [€] |
| c^{DSO} | DSO cost weight |
| C^{el} | Electricity supplier costs |
| E^{cap} | EV battery capacity [kWh] |
| E^{dem} | Daily EV energy demand [kWh] |
| k | Time instant |
| n_{EV} | Total number of EVs |
| N_h | Prediction horizon |
| n_{sc} | Total number of scenarios |
| N_s | Final time instant |
| P^{ah} | Aggregated household load [kW] |
| P^{EV} | EV charge power [kW] |
| P^g | Grid power exchange [kW] |
| P^{PV} | PV generation [kW] |
| T_s | Sampling time [h] |
| v^g | Peak power demand to grid in horizon [kW] |
| x | EV battery level [kWh] |
| z^{EV} | Positive EV power exchange [kW] |